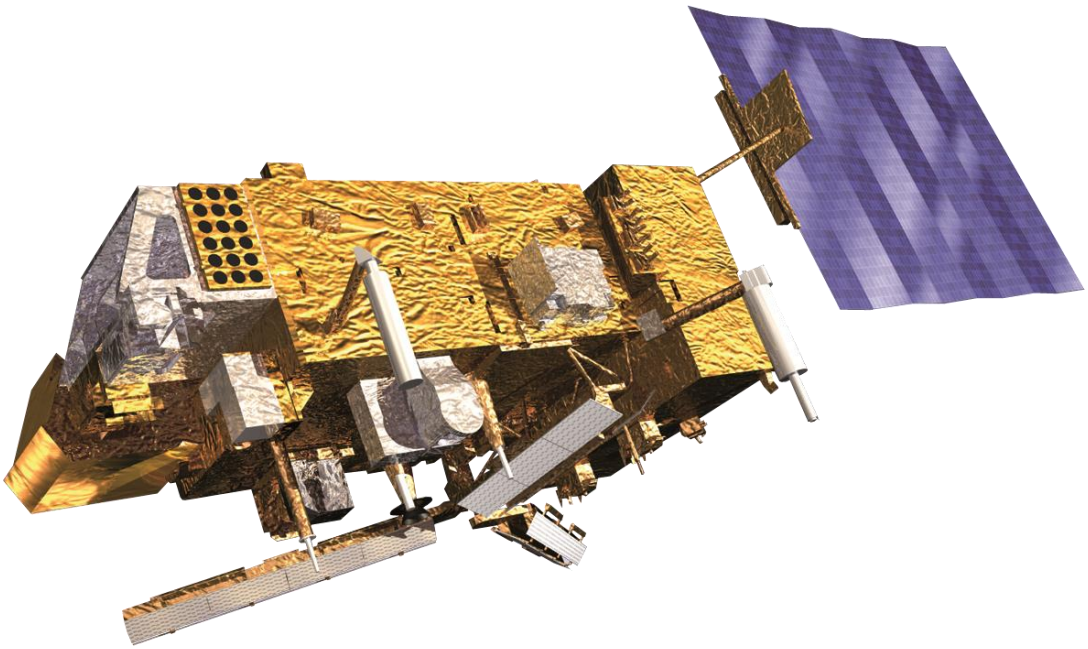

Meteorological Operational Satellite Program of Europe (MetOp-A)

Reverse engineering study

Final Report – Group 27

Authors: Group 27: Aloscari Davide, Aufiero Luca, Bono Matteo, Cappellacci Tommaso, Chaillou Adrien Pierre Camille, Stawiarska Zofia Marta

Course: Space Systems Engineering and Operations

Academic year: 2022/2023

Abstract

This document contains a detailed reverse engineering study of Meteorological Operational Satellite Program of Europe (MetOp-A). It starts with a description of objectives, functionalities and mission analysis of the satellite, and then there are detailed studies about the spacecraft's subsystems: Propulsion Subsystem PS, Tracking, Telemetry and Telecommand Subsystem TTMTC, Attitude and Orbit Control Subsystem AOCS, Thermal Control Subsystem TCS, Electric Power Subsystem EPS, Configuration and On-Board Data Handling Subsystem OBDH.

Table of Contents

1. OBJECTIVES, FUNCTIONALITIES, MISSION ANALYSIS

Change log	
§ 1.5	pp. 10: clearer definition of MetOp-A's Conceptual Operations
§ 1.5.1	pp. 10: clearer links between phases, ConOps and functionalities
§ 1.6.1	pp. 11-12: clearer goal to payloads functions correlations
§ 1.7	pp. 13: phases and functionalities more clearly reported
§ 1.8	pp. 13: justification and more detailed argumentation about used data

1.1 Mission High Level Goals

The main goals of MetOp-A mission are the observation and data services for weather prediction and climate monitoring. We can identify the following high-level goals [1.1]:

1. To ensure **continuity** and **availability** for operational purposes of **global meteorological observations** from the "morning" orbit to the global user community.
2. To provide **enhanced monitoring capabilities** (complimentary to ENVISAT) to fulfil the requirements to study the Earth climate system as expressed in several international cooperative programs such as: GCOS (Global Climate Observing System), IGBP (International Geosphere and Biosphere Program), and WCRP (World Climate Research Program).
3. To provide **continuous**, **long-term meteorological data sets**.

1.2 Mission drivers

The following drivers lead MetOp-A design [1.2]:

1. Operations:
   A. The satellite must perform global measurements and achieve **accurate global coverage** in a few days, this affects the orbit and trajectory design.
   B. A **large suite of instruments** is a significant constraint to the design of the Payload Module (PLM) and influences the total weight of the spacecraft.
   C. Potential contamination of the S/C payload by the exhaust plume is a critical condition that needs to be minimized, influencing the relations between PLM and Service Module (SVM).
2. Communications:
   A. The **continuous delivery of high-quality data** for medium- and long-term data forecasting is required, affecting the time duration of the mission, that must be interrupted when the quality is not granted anymore.
   B. It is needed to limit **electromagnetic and radio frequency (RF) interference** between the instruments and avionics, providing an effective shielding of our devices.
3. Pointing:
   A. The instruments must **point correctly and continuously at the Earth**. This will lead to three points stabilization and will affect the amount of propellant sufficient for station keeping and attitude correction maneuvers.
4. Data handling:

A. The high number of **instruments**, the big amount of **data** generated, and the **housekeeping data storage** influence the data recorder choice and TMTC design.

1.3 Mission functional analysis

Once the mission goals and drivers are understood, a **functional analysis** of the MetOp-A system must be performed in order to ensure all of the **objectives** of the mission are met. The functionalities of the system are defined before any technical solutions are developed in order to ensure the mission is successful. The main mission architecture can be seen in figure 1.1, where the mission is divided into the space and ground segments. The space segment and ground segment can then be further broken down into the architectures seen in figures 1.2 and 1.3.

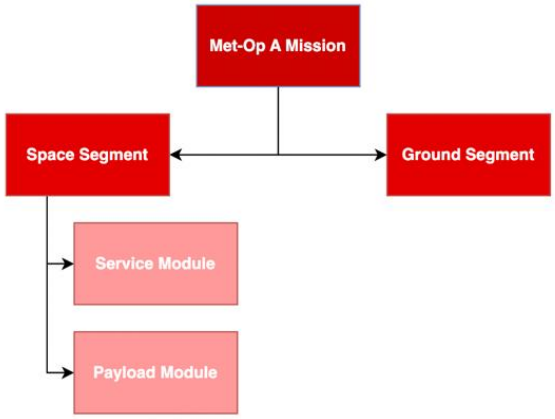

Figure 1.1: High Level Mission Architecture

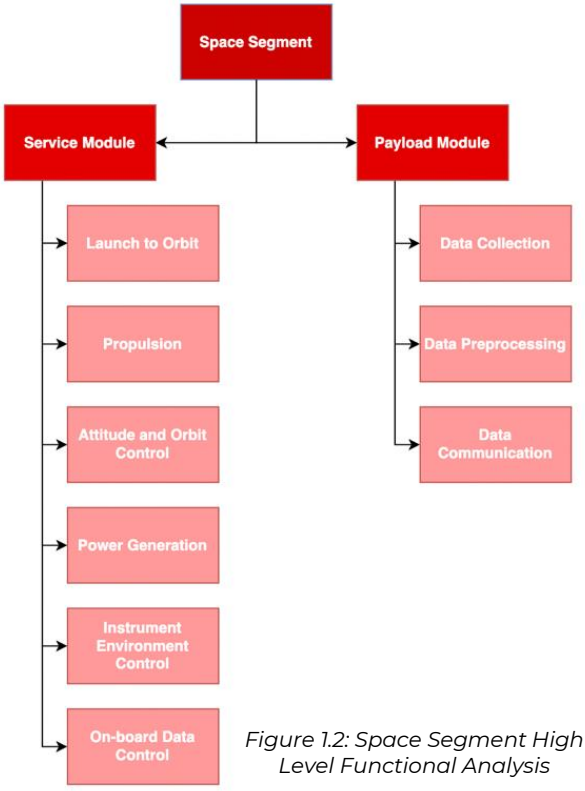

Figure 1.2: Space Segment High Level Functional Analysis

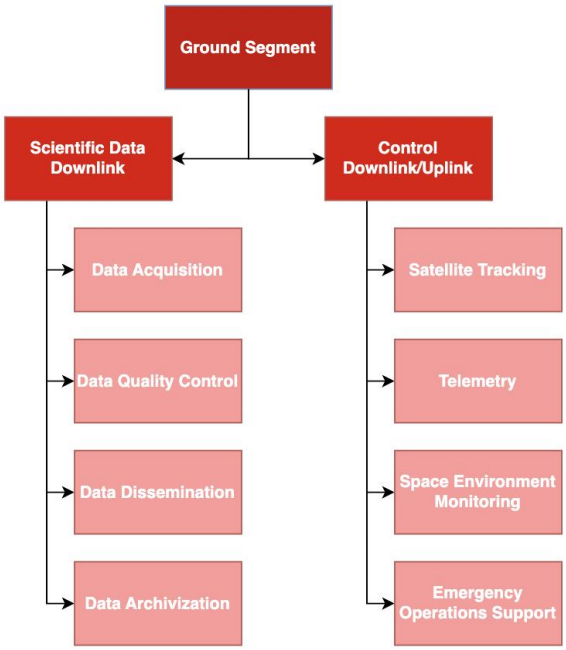

Figure 1.3: Ground Segment High Level Functional Analysis

The major functions of the MetOp-A system can be summarized as follows [1.1]:

1. Perform **global**, **continuous**, **long-term meteorological observations**:
   A. Reach an orbit that ensures global coverage;
   B. Point continuously towards the Earth to acquire data;

C. Ensure continuous power supply to the payload;
D. Maintain the instruments within their temperature, radiation, contamination operational limits.
E. Have a long operational life:
    i. perform station keeping maneuvers to counteract environment disturbances on attitude and orbital parameters;
    ii. keep pointing optimal and constant throughout the whole operational life;
F. Ensure regulation-compliant end-of-life.

2. **Enhance monitoring capabilities** of already existing Earth observation satellites:
A. Provide space for many different Earth monitoring instruments;
B. Optimize the instruments' on-board position to ensure the best operating conditions;
C. Ensure global thorough sounding:
    i. provide information about 3-D temperature and humidity fields in support of operational numerical forecasting systems,
    ii. provide ocean measurements (including surfaces stress and winds),
    iii. monitor atmospheric minor constituents,
    iv. monitor space weather conditions;
D. Ensure global thorough imagery:
    i. provide cloud imagery for forecasting applications,
    ii. estimate precipitations,
    iii. acquire sea surface temperatures (SST),
    iv. acquire clouds and Earth radiation budget temperatures,
    v. acquire sea ice information,
    vi. support the global sounding mission through the identification of cloud-free areas.

3. Promptly **supply** the acquired data to the **global user community**:
A. Pre-process the acquired data and store it until it can be downlinked;
B. Have an as continuous as possible communication with ground stations to downlink the acquired data;
C. Collect, locate and share data obtained on the ground:
    i. support WWW objectives by the reception and dissemination of in-situ observations from ocean buoys and similar data collection platforms;
D. Provide global data access:
    i. support global-scale weather forecasting by providing global data to the meteorological services within 2.25 hours of observation;
E. Provide local data access (AHRPT and LRPT):
    i. support regional weather forecasting by providing broadcasted data to local receiving stations when the satellite is in visibility;
F. Provide access to data from instruments which have not yet been declared fully operational.

1.4 Mission main phases

Mission **main phases** [1.3]:

1. Launch and early orbit phase (**LEOP**):
    A. launch;
    B. platform activation;
    C. detumbling and 3-axis stabilization;
    D. attitude correction maneuvers and deployment of solar array;
    E. ASCAT instrument antennae deployment;
    F. Telecommunication antennae deployment and start of the communication with ground;
    G. first orbital parameters determination and start of the attitude acquisition and control sequence;
    H. orbit correction maneuvers calibration and maneuver sequence optimization;
    I. out-of-plane (OOP) and in-plane (IP) maneuvers to reach the desired orbit;
    J. Earth-pointing.
2. Satellite In-Orbit Verification (**SIOV**) [1.4]:
    A. satellite initial characterization based on house-keeping telemetry received in S-band;
    B. payload module switch on in operational mode and first tests of science data continuity and format;
    C. characterization of Service Module SVM, Payload Module PLM and Instrument Control Unit switch-ons;
    D. instruments switch-on and in-orbit verification of the instruments.
3. Eumetsat Polar System (**EPS**) **verification** and **validation** phase:
    A. verification and validation of the main EPS ground system functions, data flows, links and services to the users:
        i. characterisation of the space-to-ground links (S-band, X-band, HRPT, LRPT),
        ii. HRPT/LRPT local broadcast service verification,
        iii. verification of the Level-0 raw data archive & retrieval service,
        iv. Level-0 data transfer to the partner organisations,
        v. Global Telecommunication System readiness,
        vi. NOAA cross-support services establishing,
        vii. Search & Rescue, Data Collection System Level-0 and Space Environment Monitor Level-0 services verification;
    B. calibration and validation activities for the centrally generated EPS products:
        i. geo-location and radiometry of the Level-1 products verification,
        ii. Level-1 products validation and processing parameters optimization,
        iii. Level-2 products validation and release.
4. **Scientific operations**:
    A. station keeping maneuvers for keeping optimal orbit and attitude;
    B. communication, telemetry retrieval and telecommands delivery;
    C. nominal payload operations and final products delivery.
5. **Disposal**.

1.5 Conceptual Operations

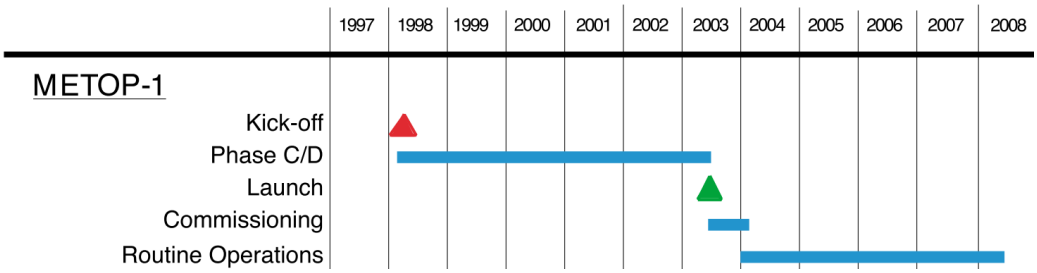

Figure 1.4: MetOp-A ConOps Gantt Chart

MetOp-A **conceptual operations** [1.5]:

1. Project kick-off.
2. Phases C and D (102 months): design, development, building, integration, verification and testing.
3. Launch.
4. Commissioning:
    A. LEOP (4 days);
    B. SIOV (5 months);
    C. EPS verification and validation (1 month).
5. Routine operations (60 months).
6. Disposal (atmospheric re-entry within 25 years after the end of operations).

1.5.1 Phases links to ConOps and functionalities

1. **LEOP phase**: linked to *launch and commissioning* ConOps; *meteorological observations, enhanced monitoring capabilities and global data supply* functionalities.
2. **SIOV phase**: linked to *commissioning* ConOp; *long operational life, global thorough sounding and imagery* functionalities.
3. **EPS verification and validation phase**: linked to *commissioning* ConOp; *global thorough sounding, imagery and data supply* functionalities.
4. **Scientific operations phase**: linked to *routine operations* ConOp; *meteorological observations, global thorough sounding, imagery and data supply* functionalities.
5. **Disposal phase**: linked to disposal ConOp and *regulation-compliant end-of-life* functionality.

1.6 On board scientific instruments primary utilization

There are **eleven on board scientific instruments** for the MetOp-A mission, each with its own primary utilization [1.1][1.2]:

1. Microwave Humidity Sounder (MHS):
    - Measures microwave radiation from the Earth's surface which quantifies at various altitudes humidity (rain, snow, hail, sleet, temperature).
2. Advanced Very High-Resolution Radiometer (AVHRR/3):
    - Used for imaging of land, water, and clouds and measures sea surface temperature, ice, snow, and vegetation cover using 6 spectral bands.

3. Advanced Data Collection System (ADCS-3 or Argos-3):
    - In charge of data collection and location, specifically with the ADCS, and relays this information to ground segments.
4. Search and Rescue Processor and Repeater (SARP and SARR):
    - Radiolocation system for search and rescue operations which helps relay emergency radio signals to ground stations from individuals in distress.
    - Preprocesses data for transmission back to ground.
5. Space Environment Monitor (SEM-2):
    - Spectrometer that measures intensity of Earth's radiation belts and flux of charged particles at the satellite's altitude.
    - Warns of solar wind occurrences that can affect all satellites.
6. Advanced Microwave Sounding Units (AMSU-A):
    - Measures scene radiance in microwave spectrum and works with HIRS to make temperature and humidity profiles of upper stratosphere.
7. Global Ozone Monitoring Experiment-2 (GOME-2):
    - Spectrometer that collects light arriving from Sun either reflected in atmosphere or from a direct view and decomposes it into spectral components to get a detailed picture of atmospheric content and a profile of the components.
8. Global Navigation Satellite System Receiver for Atmospheric Sounding (GRAS):
    - Collects data of temperature and humidity of atmosphere using atmospheric sounding and GPS radio occultation.
9. Advanced SCATterometer (ASCAT):
    - Measures wind speed and direction over ocean using scatterometers and contributes to land and sea ice monitoring, soil moisture, snow properties, and soil thawing.
10. High-resolution Infrared Radiation Sounder (HIRS/4):
    - Measures radiance in IR spectrum to work with AMSU to calculate surface radiance, ozone levels, atmospheric temperature, precipitation, pressure, and humidity up to the upper stratosphere.
11. Infrared Atmospheric Sounding Interferometer (IASI):
    - Measures IR radiation emitted from Earth's surface to measure humidity and atmospheric temperature in the troposphere and lower stratosphere as well as chemical profile of components related to climate monitoring.

1.6.1 Goal to payloads functions correlations

All the on-board instruments correlate to **meteorological observation**, **monitoring**, and **data providing functions** of the MetOp-A satellite, but more specifically:

1. Microwave Humidity Sounder (MHS)
    - *2.C.i* provide information about 3-D temperature and humidity fields in support of operational numerical forecasting systems, *2.D.iv* acquire clouds and Earth radiation budget temperatures.
2. Advanced Very High-Resolution Radiometer (AVHRR/3)
    - *2.C.i* provide information about 3-D temperature and humidity fields in support of operational numerical forecasting systems, *2.C.ii* provide ocean

measurements (including surfaces stress and winds, *2.D.i* provide cloud imagery for forecasting applications, *2.D.iii* acquire sea surface temperatures (SST), *2.D.v* acquire sea ice information.

3. Advanced Data Collection System (ADCS-3 or Argos-3)
    - *1.E.ii* keep pointing optimal and constant throughout the whole operational life, *3.A* pre-process the acquired data and store it until it can be downlinked, *3.B* have an as continuous as possible communication with ground stations to downlink the acquired data.
4. Search and Rescue Processor and Repeater (SARP and SARR)
    - *3.A* pre-process the acquired data and store it until it can be downlinked, *3.B* have an as continuous as possible communication with ground stations to downlink the acquired data.
5. Space Environment Monitor (SEM-2)
    - *2.C.iv* monitor space weather conditions, *2.D.iv* acquire clouds and Earth radiation budget temperatures.
6. Advanced Microwave Sounding Units (AMSU-A)
    - *2.C.i* provide information about 3-D temperature and humidity fields in support of operational numerical forecasting systems.
7. Global Ozone Monitoring Experiment-2 (GOME-2)
    - *2.C.iii* monitor atmospheric minor constituents.
8. Global Navigation Satellite System Receiver for Atmospheric Sounding (GRAS)
    - *2.C.i* provide information about 3-D temperature and humidity fields in support of operational numerical forecasting systems, *2.D.i* provide cloud imagery for forecasting applications, *2.D.ii* estimate precipitations.
9. Advanced SCATterometer (ASCAT)
    - *2.C.ii* provide ocean measurements (including surfaces stress and winds), *2.D.v* acquire sea ice information.
10. High-resolution Infrared Radiation Sounder (HIRS/4)
    - *2.C.i* provide information about 3-D temperature and humidity fields in support of operational numerical forecasting systems, *2.D.i* provide cloud imagery for forecasting applications, *2.D.ii* estimate precipitations, *2.D.iv* acquire clouds and Earth radiation budget temperatures, *2.D.vi* support the global sounding mission through the identification of cloud-free areas.
11. Infrared Atmospheric Sounding Interferometer (IASI)
    - *2.C.i* provide information about 3-D temperature and humidity fields in support of operational numerical forecasting systems, *2.C.iii* monitor atmospheric minor constituents.

1.6.2 Payload to ConOps/phases correlations

Payload functionalities are tested and started during the commissioning phases (1-3) of the mission. Deployment of the instruments occurs in the LEOP (1) and SIOV (2) phases and then data collection and relay occur during the routine operations phase (4).

1.7 Functionalities/phases to trajectory design correlations (Mission Analysis understanding)

MetOp-A **mission analysis** [1.1]:

1. Phase 1 *LEOP*, functionality 1.A *reach an orbit that ensures global coverage* -> MetOp-A will perform its scientific operations in an inclined orbit with an angle of 98.7° to the Equator, at an altitude of 817 km. It takes about 100 minutes to complete one orbit, in the meantime the Earth has rotated around 25° which means observations are made over a different section of the Earth in each orbit. In this way it's possible to achieve complete global coverage within five days.
2. Phase 4 *scientific operations*, functionality 1.C *ensure continuous power supply to the payload* -> Sun-synchronous polar morning orbit.
3. Phase 4 *scientific operations*, functionalities 1 *global, continuous, long-term meteorological observations*, 2.C-D *ensure global thorough sounding and imagery*, 3 *supply the acquired data to the global user community* -> station keeping maneuvers for keeping orbit, optimal attitude and pointing.

1.8 Reverse study of the trajectory design per phase towards the Δv budget justification and retrieval

Phase 1.A is performed by Fregat upper stage:

- First burn: 1299.35 m/s, fuel consumed: 2771 kg;
- Second burn: 182.1 m/s, fuel consumed: 314 kg;
- Third burn: 237.7 m/s, remaining fuel consumed.

These maneuvers are performed by the last stage of the rocket that brings MetOp-A to orbit, and so they don't affect its propulsion subsystem fuel and Δv capabilities [1.1].
Immediately after the release of the satellite from the rocket's last stage, **out-of-plane** (OOP) and **in-plane** (IP) **maneuvers** must be performed to reach the desired orbit (1.56 m/s Δv OOP, 2.558 m/s Δv IP) [1.3].
When the satellite has a non-zero angular velocity, a maneuver called **de-tumbling** is performed, with an estimated cost between 2-6 m/s per year [1.7].
Since the spacecraft needs to always **point at the Earth surface** some fuel is spent to maintain the attitude during its operational life (estimated cost between 0.1-7 m/s [1.7]).
Another important factor is that in Low Earth Orbit **Drag** is relevant like other environmental disturbances such as **Magnetic Field** and **Gravity Gradient**. All these factors induce external forces and torques that must be compensated, and in terms of velocity, considering the data acquired on the disturbances faced by similar satellites to MetOp-A orbiting in a similar LEO [1.6], it costs about 25 m/s per year [1.7].
Considering an operational life of 5 years [1.5], in the worst-case scenario the **total Δv** MetOp-A must be able to perform, considering the aforementioned data estimated from similar satellites in LEO, given by ECSS standards and the simulated OOP and IP maneuvers, is **166 m/s**.

2. PROPULSION SUBSYSTEM

2.1 Mission propulsion architecture

To answer the requested **Δv budget**, **eight pairs of thrusters** are used. Each pair comprise the main thruster and its redundant one.Each thruster uses **Hydrazine** (**N_2H_4**) as liquid monopropellant and is designed to deliver a nominal thrust of **22.7 N**. Moreover, the thrust provided is in the form of **pulses** and designed to operate at 8 Hz.

The **propellant mass** is **M_{fu} = 316 kg**, stored in **four pressurized tanks** (including residual). The propulsion subsystem works in **blow-down** mode and its other components are four latch valves, pressure transducers, fuel, and gas valves for the propellant/pressurant loading/off-loading and pressurizing/venting.

In Figure 2.2, a graphical view of the thruster pairs configuration is given. The cartesian reference frame indicated in the figure depicts the satellite body frame of reference in which –Z points toward the Earth center. The rectangular box on the left in Figure 2.2 represents the spacecraft and the green patches show the locations of the **thruster pairs grouping** on the spacecraft.

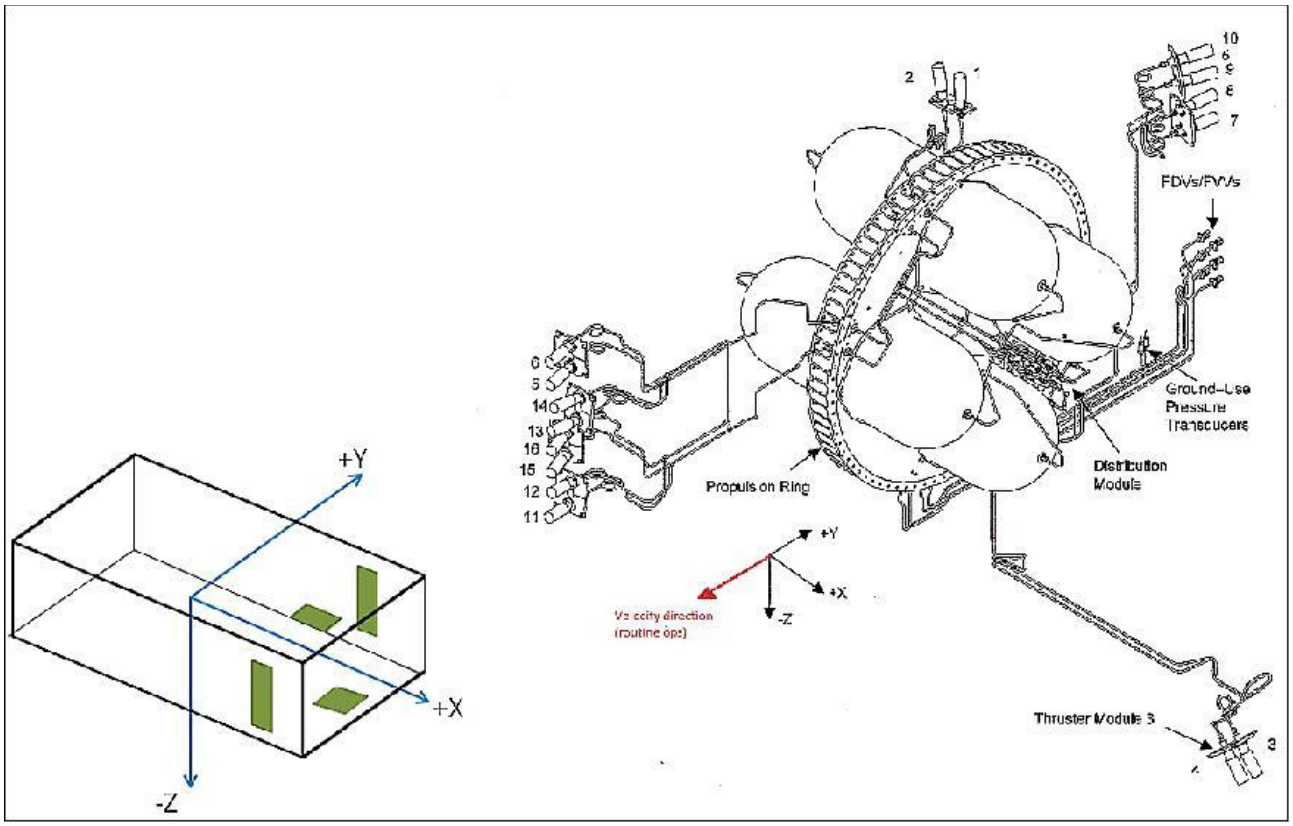

Figure 2.2: MetOp-A thrusters configuration and location

Among the eight thrusters, four are dedicated to **propulsion in the ± Y axis**, while all of them contribute to the generation of **torque**, leading to a **rotation control in all three axes**. Table 2.1 shows the thruster function according to its number.

Thruster N° (Main-Redundant)	Thruster function
1-2	Torque (+Y)
3-4	Torque (-Y)
5-6	Torque (-X)
7-8	Torque (-Z); Thrust (-Y)
9-10	Torque (+Z); Thrust (-Y)
11-12	Torque (+X)
13-14	Torque (+Z); Thrust (+Y)
15-16	Torque (-Z); Thrust (+Y)

Table 2.1: Thruster module configuration and function

During the propulsion phase, the imbalance in the torque due to changes in the center of mass causes one of the propulsion thrusters to pulsate less than the other. A similar imbalance in the torque and thrust applies to the slew and anti-slew maneuvers as well. Throughout the maneuver phase, the attitude control thrusters are actively controlled by the AOCS to correct the attitude pointing due to torque imbalance created by the propulsion and coupled thrusters [2.1][2.2].

2.2 Primary and secondary propulsion

- Primary propulsion: thrusters N° 7-8, 9-10, 13-14, 15-16, used for **orbital corrections maneuvers** after the release of the satellite from the rocket's last stage (orbit trim), and during the whole lifetime of the spacecraft.
- Secondary propulsion: all the thrusters providing **torque**, used for **station keeping** and **reaction control system** (attitude control, de-tumbling, pointing, environmental disturbances compensation).

2.3 Propulsion type and architecture rationale

As the most important and demanding orbit insertion maneuvers are performed by Fregat upper stage, that brings MetOp-A almost to its definitive orbit, the satellite's propulsion subsystem is devoted to **orbit correction maneuvers**, **station keeping** and **attitude control** throughout its whole operational life. For this reason, it consists of many thrusters which provide **low thrust** in the form of **pulses**. All of them provide **torque**, allowing a complete and precise three-axis control of the spacecraft; four of them can provide **thrust**, only in the ± Y direction, as it's needed just for the starting orbit trim maneuvers in the LEOP phase and to counteract the drag generated by LEO environmental disturbances during the scientific operations phase.

The **Δv** MetOp-A's propulsion subsystem shall provide throughout its 5 years of scientific operations is **166 m/s**: 1.56 m/s out-of-plane and 2.558 m/s in-plane maneuvers to reach the desired orbit after separation from the last rocket stage [2.3], 6 m/s per year for de-tumbling, 7 m/s for precise Earth pointing, 25 m/s per year for environmental disturbance forces and torques compensation. All the Δv shall be delivered in the form of **low-thrust**, **precise correction maneuvers**, most of which concern torque rather than thrust. These considerations led to the aforementioned MetOp-A propulsion architecture, optimized to meet the Δv budget.

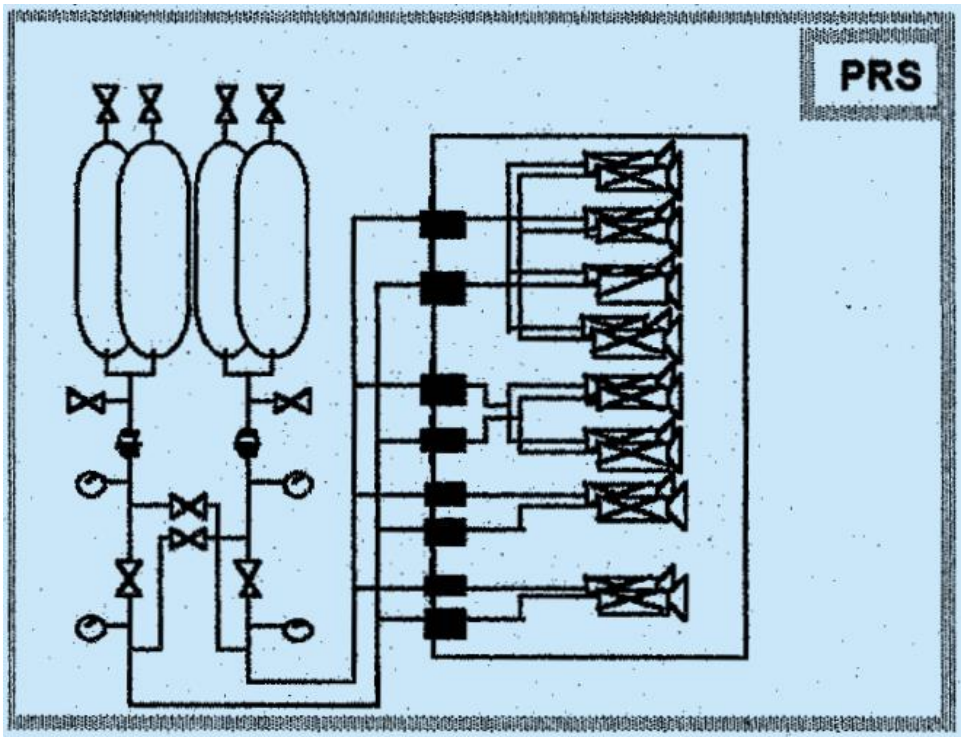

Figure 2.3: MetOp-A propulsion subsystem schematic representation

The **blowdown monopropellant** (hydrazine) **propulsion subsystem** used in MetOp-A is **cheap**, **simple** and **reliable**, sufficient to provide the **low thrust** needed, able to meet the **multiple starts** and **pulsing** requirements, compatible with the **5 years lifetime**; pressure, thrust and mass flow variation with time caused by the blow down pressurization system doesn't affect the ability of the propulsion subsystem to cope with MetOp-A requirements throughout its lifetime.

2.4 Reverse sizing

To perform the reverse sizing of the propulsion system, a MATLAB code was developed; it allowed for comparison of **eight configurations of the propulsion subsystem**. The simulation then provided several important outputs, most importantly the sized total mass of the propulsion system. A notable finding was that although for the cylindrical configuration of the tanks many heights were tested, the result variation between heights was so small that it was decided that the height and radius combination would be determined by spatial constrains and mean values would be used for trade-off analysis.

Starting with a **dry mass** of **3769 kg**, the **mass** of the **propellant** was found to be **478.9 kg**. From this the mass of the propulsion system is derived through simulation. Certain values are found to be the same for all configurations such as initial pressure of the pressurizing gas is 6.75 MPa, volume of the gas is 0.1304 m^3, volume of each of the four tanks is 0.1646 m^3, and the volume of the propellant is 0.5216 m^3. The most important changing values are summarized in the **decision matrix** below. Ratings are given on a scale of 1-5.

System Configuration	Variable Considered							
	Mass of Pressurized Gas in kg		Cost of Tank in €			Mass of Propulsion System in kg		**Total**
	Value	Rating	Mass Value	Estimated Cost[1]	Rating	Value	Rating	
A (He, Ti, Spherical)	1.735	5	4.895	33.33	2	36.119	5	**12**
B (He, Ti, Cylindrical)	1.735	5	6.527	44.45	1	43.298	4	**10**
C (He, Al, Spherical)	1.735	5	9.374	21.56	5	55.827	3	**13**
D (He, Al, Cylindrical)	1.735	5	12.499	28.75	4	69.576	2	**11**
E (N_2, Ti, Spherical)	12.145	2	4.895	33.33	2	47.57	4	**8**
F (N_2, Ti, Cylindrical)	12.145	2	6.527	44.45	1	54.749	3	**6**
G (N_2, Al, Spherical)	12.145	2	9.374	21.56	5	67.279	2	**9**
H (N_2, Al, Cylindrical)	12.145	2	12.499	28.75	4	81.027	1	**7**

Table 2.2: MetOp-A propulsion subsystem decision matrix

Given this matrix, configurations A, C, and D are to be considered as the most viable options. What follows is a discussion of the factors that ultimately lead to the **selection of configuration D** with Helium as the pressurant gas, Aluminum as the tank material, and a cylindrical tanks shape.

2.4.1 Propellant selection and masses

- The main drivers that guided the choice of the propellant subsystem are **reliability**, **simplicity**, **cheapness** and **compactness**, over other parameters like maximum thrust, specific impulse and performance. This led to the choice of a **monopropellant** system rather than a bipropellant one.
- Because of motivation to produce a reliable propulsion subsystem, **hydrazine** is chosen as the best propellant option as it is already widely used as a monopropellant, very stable, with a sufficient I_{sp} of 230 s, and it's a cheap solution.
- Reverse sizing calculations of the **mass** of the **propellant** yield 478.9 kg which is 151.5% of the 316 kg that were used on MetOp-A. Discrepancy is present because the calculations performed used **conservative margins** [2.4] such as 20% for the Δv, 5.5% for loading, uncertainty, and residual mass of the propellant, and 10% for unusable volume of the propellant. MetOp-A engineers used less margins due to the similarity of MetOp-A's propulsion subsystem to the flight-proven ones of many satellites.

[1] Calculated using a cost of 6,81 €/kg for Titanium and 2,30 €/kg for Aluminum [2.5]

2.4.2 Tanks sizing (propellant/pressurant), number, material adopted

- Spherical tanks tend to yield lower masses, but cylindrical tanks can achieve a much wider array of possible radius and height combinations to fit the available space inside of the spacecraft while still maintaining the same volume and a comparable mass. For this reason, **1 m tall cylindrical tanks** are chosen, and the performed calculations yield a **22.8 cm radius**.
- **4 tanks** are used for redundancy as well as to create a symmetric loading on the spacecraft to balance the feeding system to all the thrusters. Having 4 tanks also lowers blow down system pressure losses over time.
- Both aluminum and titanium can withstand the pressure with an acceptable thickness of around 2 mm as well as the chemical properties of hydrazine; **Aluminum** is **cheaper** than titanium and although the latter is lighter, the cost of an aluminum tank is half of the titanium tank without significant difference in the material properties.

2.4.3 Pressurant selection and masses

- Helium and nitrogen are both used as pressurant gas in many space propulsion subsystems. Sizing differences are present in the mass of the pressurant as the nitrogen is about 7 times as dense as the helium and therefore **helium** can provide **better mass performance**.

2.4.4 Feeding strategy selection and sizing

- **Blow down pressurization system**: **cheap**, **simple** and **reliable**; thrust and mass flow variation with time doesn't affect the ability of the propulsion subsystem to cope with MetOp-A requirements throughout its lifetime.
- **20% margin** for mass of the pressurant, **1%** for volume due to the bladder, and **10%** to account for the cables are used for the design of the propulsion subsystem [2.4].

2.4.5 N° and positioning of thrusters

- **16**: **8 main thrusters** and **8** ones for **redundancy**; they provide torque around the three axes, leading to a complete rotation control, and thrust in the ± Y axis, sufficient for MetOp-A station keeping.
    - The thrusters used were the MONARC 22-6 [2.6] which have an individual dry mass of 0.72 kg with a specific impulse of 230 s.

Figure 2.4: MetOp-A thrusters

2.4.6 Positioning of tanks and lines in the configuration

- **4 tanks** located **close to the center of mass** of the spacecraft, so that fuel mass reduction with time doesn't affect the position of the center of mass. Lines are placed in a **cross-feed** configuration for **redundancy**, and they are as short as possible, with thrusters located close to the tanks, to **reduce pressure losses**. A machined aluminum alloy plate, the **propulsion module ring**, is used to support the four propellant tanks and to interface with both the Payload Module and the Service Module central structure.

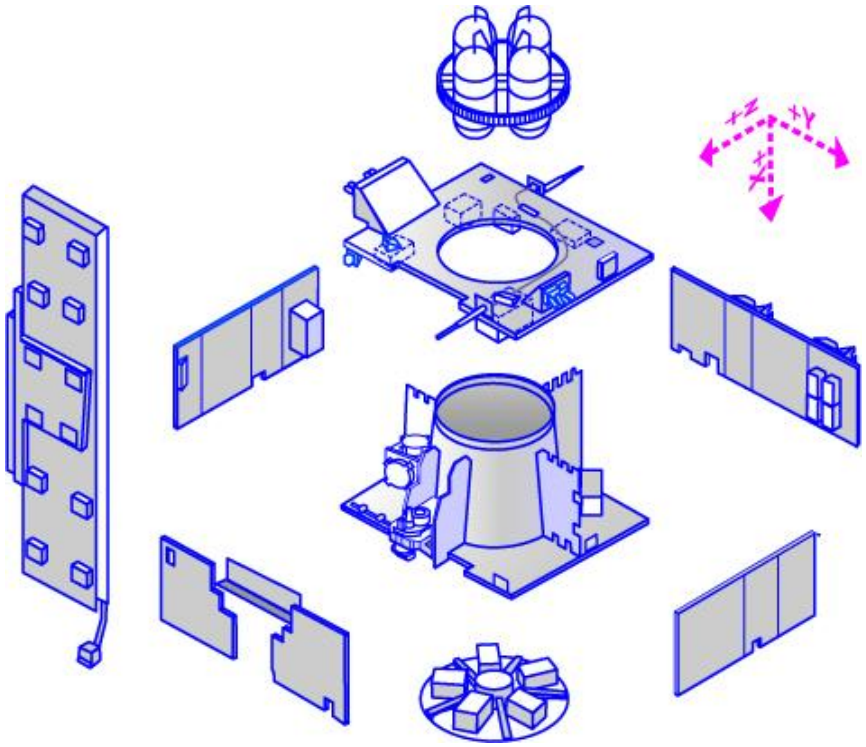

Figure 2.4: Exploded view of MetOp-A Service Module with tanks and propulsion module ring

3. TRACKING, TELEMETRY AND TELECOMMAND SUBSYSTEM

3.1 MetOp-A TTMTC architecture and solutions for subsystem design

For RF communication, MetOp-A employs an omnidirectional **S-band** coverage that provides TT&C support (**uplink 2 kbit/s**, **downlink 4 kbit/s**). Instrument data is downlinked in **X-band** at a rate of **70 Mbit/s**. Onboard **storage capacity** of **24 Gbit** (solid state recorder with a data rate of 70 Mbit/s) is provided. In addition to onboard recording and X-band downlink capabilities, MetOp-A supports the real-time broadcast of instrument data to local authorized users by the following means:

- **LRPT** (Low-Rate Picture Transmission) links with **72 kbit/s** in **VHF-band** for selected instrument data.
- **AHRPT** (Advanced High-Rate Picture Transmission) links with **3.5 Mbit/s** in **L-band**. The new AHRPT service (a WMO standard) enables regional users to receive all data relevant to their area in real time. Users operating existing HRPT stations will have to modify their stations to receive the "Advanced" MetOp data.

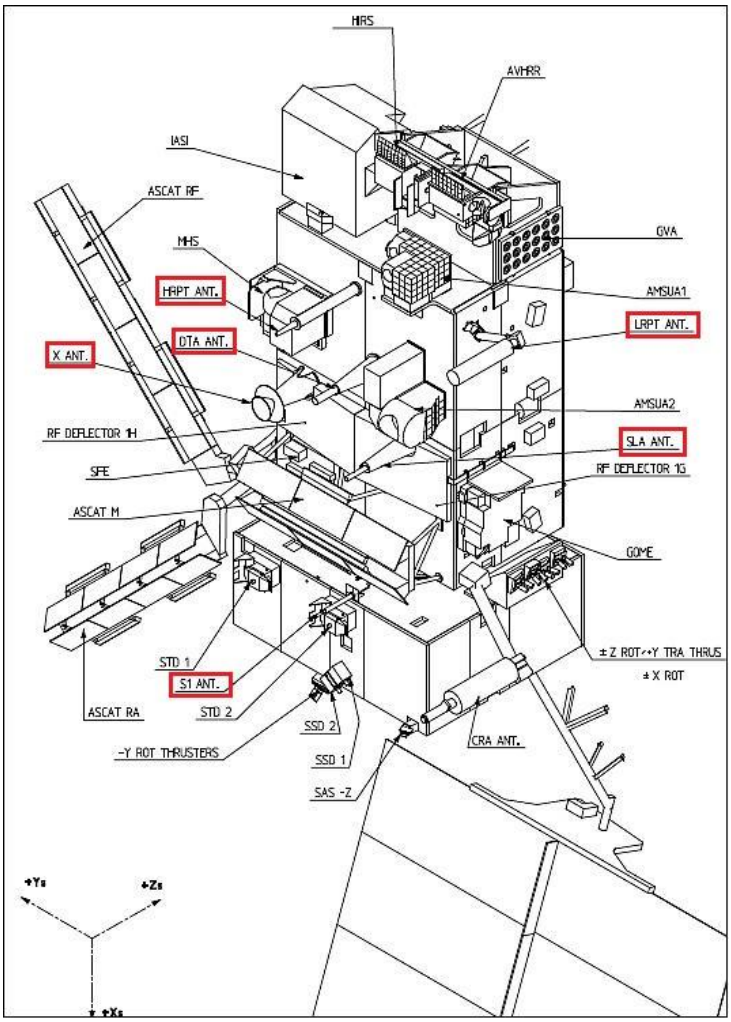

Figure 3.5: Line drawing of the MetOp-A spacecraft with antennas highlighted [3.2]

Global coverage of the measurement data is achieved by a **recording** of all **measurement data** over a **complete orbit** from ground station to ground station. Like the Environmental Satellite (ENVISAT) and Cluster, a **solid-state recorder** (SSR) is used to do this. **Simultaneous recording and dumping** is supported such that special measures to avoid data losses during down-link are not required. At each **ground station** pass the **recorder** can be **dumped** as far as the actual recording position, i.e. also measurement data acquired during the pass can immediately be down-linked within the same pass. The SSR memorization is **sufficient** to provide the necessary **internal redundancies** as well as to cover **worst case down-link** scenario.

Data type	Frequency Domain	Modulation Scheme	Data Rate	Bandwidth
TT&C uplink	S-band, 2053.4 MHz	NRZ/PSK/PM	2 kbit/s	1500 kHz
TT&C downlink	S-band, 2230 MHz	SP-L/PSK/PM	4 kbit/s	2000 kHz
Global data dump	X-band, 7.8 GHz	QPSK	70 Mbit/s	63 MHz
LRPT downlink	VHF-band, 137.1 MHz	QPSK	72 kbit/s	150 kHz
AHRPT downlink	L-band, 1701.3 MHz	QPSK	3.5 Mbit/s	4.5 MHz

Table 3.3: Summary of MetOp-A communication links with the ground segment [3.1][3.5]

3.1.1 Ground segment

The **EPS** (Eumetsat Polar System) **Ground Segment** includes all the ground facilities required to support the orbiting MetOp satellites and the EPS mission, including both normal and degraded mission modes. Its objectives are:

- To ensure that the satellites perform their mission nominally.
- To perform the ground operations to fulfil the global mission, acquiring and processing the global data received from the NOAA and MetOp satellites and disseminating the processed data to the Eumetsat member states. This includes product quality control, data archiving, and provision of user services.
- To perform all the ground operations to support the local data-access mission (HRPT/LRPT).
- To support NOAA for global data acquisition and telemetry, tracking and control during blind orbits of the NOAA ground segment (and on request for specific operations).
- To support the space environment monitoring and data-collection missions.

The **core ground segment** provides the following functions at the different sites:

- Central Site, at Eumetsat headquarters in Darmstadt, Germany, includes all the functions for monitoring and controlling the satellite and the ground segment. Included are the generation of the centrally extracted products and their dissemination.
- The Polar Site, at Svalbard (latitude 78° N) [3.4], hosts the CDA (Control & Data Acquisition) station that receives the MetOp recorder dump every orbit and command the satellite. The CDA also receives NOAA satellite data dumps when they are beyond their own stations.
- The BUCC (Back-Up Control Center) site, close to Madrid, Spain, was created in case of major problems with the central site.

3.2 TTMTC type and architecture rationale (according to operations/phase and data volume to transfer space to ground)

The MetOp-A satellite is in continuous communication with ground through all phases of its mission. During the **LEOP** phase, the antennae are deployed and communication especially through the S-band begins. During the **SIOV**, the S-band communication is especially pertinent as it allows for the satellite initial characterization using the telemetry provided by the S-band antenna, and the first tests of science data are conducted so X-band, LRPT, and AHRPT also become active. During the **EPS verification and validation** phase a thorough check of all the communication is performed. During the **scientific operations** all the instruments continue to be used to relay information and scientific data back to the Earth [3.10].
The architecture of the TTMTC had to be divided into **4 separate links** to allow for separation of satellite operations and scientific operations. This is to ensure that all necessary data is transmitted **without delay** and **to not overload** the transmission system. Also, the amounts of data rate required for the instrument data, especially imaging data, calls for architecture that is capable of much **higher data rates** than for TT&C communication. The differences in frequency domains also allow for **reduced interference** across communications as well as **larger capacity of transmission** as all different types of data can be communicated at the same time without overloading the architecture. The different parts of the system also allow for **redundancy** as even though each link has a dedicated purpose, if necessary, the data can be transmitted back to the ground through other means [3.1].

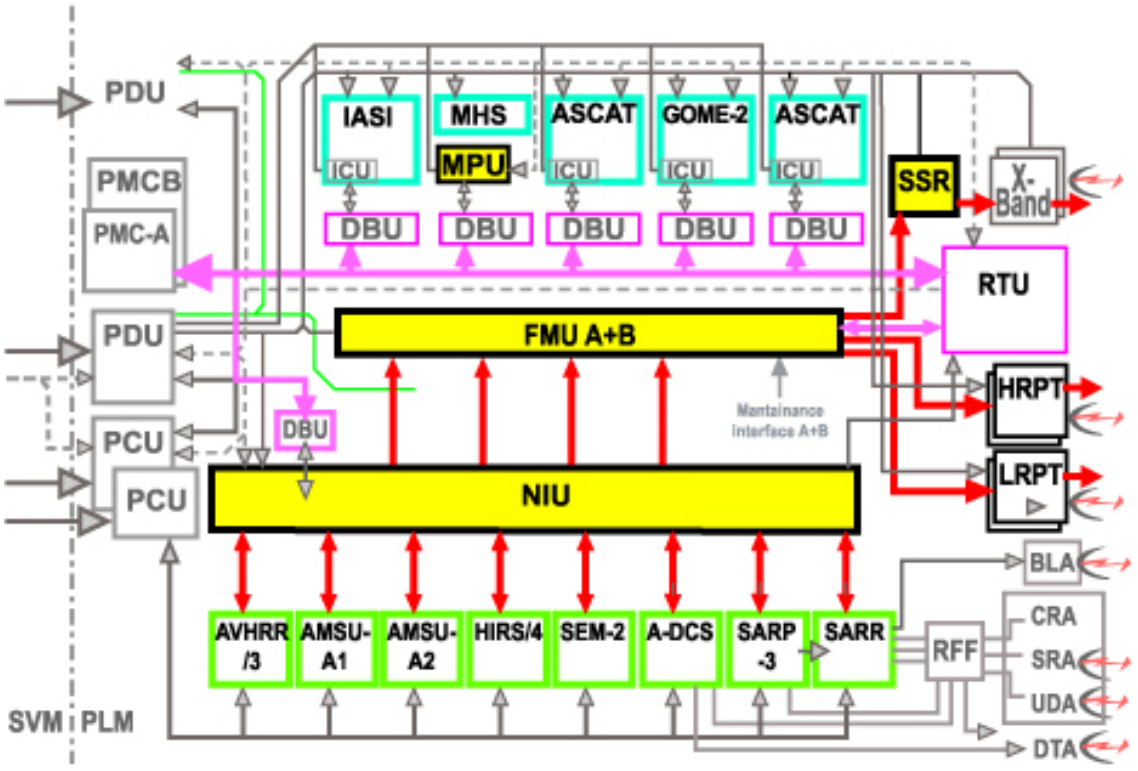

Figure 3.6: Overview of PLM measurement data acquisition, handling, storage and downlink

The total **scientific instruments data rate** is 7.5 kbit/s (ADCS) + 2.1 kbit/s (AMSU-A1/A2) + 60 kbit/s (ASCAT) + 622 kbit/s (AVHRR/3) + 40 kbit/s (GOME-2) + 60 kbit/s (GRAS) + 2.9 kbit/s (HIRS/4) + 1500 kbit/s (IASI) + 3.9 kbit/s (MHS) + 2.4 kbit/s (SARP-3/SARR) + 0.166 kbit/s (SEM-2) = **2301 kbit/s** [3.9]. Considering an orbital period of 101.4 minutes, the total **amount of data** collected by MetOp-A scientific instruments in one orbit is **14 Gbit**, that can be stored inside the onboard storage of 24 Gbit, together with the much smaller amount of telemetry gathered in the meantime. Considering the 70 Mbps data rate for global data dump, the data collected in one orbit can be downlinked in **200 seconds**; this time lies within the 12 minutes communication window MetOp-A has with Svalbard ground station in each orbit [3.11]. In the same 200 s time span the satellite can downlink **819 kbit** of **telemetry** data, and the ground station can uplink **400 kbit** of **telecommands and ranging** data.

3.3 Reverse sizing

	Global data dump	TT&C uplink	TT&C downlink
Frequency	7.8 GHz	2053.4 MHz	2230 MHz
Bandwidth	63 MHz	1500 kHz	2000 kHz
Data rate	70 Mbps	2 kbps	4.096 kbps
Input power	90 W	-	30 W
Transmitted power	50.4 W 17.02 dBW	20000 W 43.01 dBW	4.5 W 6.53 dBW
Modulation	QPSK	QPSK	QPSK
Encoding	R-S	R-S	R-S
Minimum Eb/N0	5.5 dB + 3 dB margin	5.5 dB + 3 dB margin	5.5 dB + 3 dB margin
Tx gain	10.7 dB	39.9 dB	1 dB
Rx gain	51.5 dB	0.3 dB	40.6 dB
Losses	-186.35 dB	-169.31 dB	-170.03 dB
EIRP	25.7 dB	81.9 dB	6.5 dB
Received power	-107.15 dB	-86.09 dB	-121.86 dB
System noise density	-204.62 dB	-204.62 dB	-204.62 dB
Eb/N0	**21.46 dB**	**87.96 dB**	**49.08 dB**
Carrier power	-113.17 dB	-99.74 dB	-127.88 dB
SNR margin	**3.46 dB**	**33.12 dB**	**3.74 dB**

Table 3.4: MetOp-A X-band and S-band link budget computation [3.1-3.8]

3.3.1 Frequency selection, data rate, band

- X-band: frequency **7.8 GHz**; data rate **70 Mbps**; band **63 MHz**. These high values allow the downlink of all the scientific data collected in one orbit of acquisition by all the instruments on board MetOp-A in the short amount of communication time the satellite has with Svalbard ground station.
- S-band: widely used band for communications with satellites. Frequency: **2053.4 MHz** uplink, **2230 MHz** downlink; data rates: **2 kbps** uplink, **4.096 kbps** downlink; bands: **1500 kHz** uplink, **2000 kHz** downlink. It is a much lower data rate than the instrument data connections as volume information such as images is not transmitted here and on-board pre-processing reduces what needs to be sent.

3.3.2 Signal manipulation (encoding, modulation)

- X-band / S-band: **Reed-Solomon** encoding, **QPSK** modulation. Optimized to have enough data-rate, with a not too high Eb/N0 minimum. R-S encoding is standardly used for telemetry.

3.3.3 Antenna selection, type, characteristics and number correlated to which frequency and for which data transfer

- X-band: a **parabolic reflector antenna**, capable of reaching the high gain needed for scientific data downlink.
- S-band: a **tubular monopole low gain antenna**, cheap, simple, with bad performances but still sufficient to meet telemetry transmission and telecommands and ranging reception low requirements; it is omnidirectional, to be able to send telemetry and receive telecommands also in non-nominal pointing situations.

3.3.4 Ground station selection: where, which size/frequency/data rate

- **Svalbard ground station**, at a latitude of 78°N, has a 11 m dish parabolic reflector antenna both for X-band and S-band communication, and it has a communication window with MetOp-A each polar orbit the satellite performs around the Earth, allowing enough data downlink per orbit not to overload MetOp-A's internal data storage.

3.3.5 Amplifier selection

- X-band: **Travelling Wave Tube Amplifier** (TWTA), preferred for the high 90 W power.
- S-band: **Solid State Amplifier** (SSA), lighter and better for lower power (30 W).

3.3.6 Contact strategy: contact windows duration and data volume transferred per contact (average)

- X-band: downlinked nominally to 2 ground stations and the data must be downlinked no later than one orbit after recording (about 2.25 hours).
- S-band: Routine operation commands are uplinked about 36 hours before execution and contact with CDA occurs about once each orbit.
- LRPT and AHRPT provide real time broadcasting of data, so the contact window is continuous, and all ground stations can download it.
- MetOp-A has **one contact window per orbit** with Svalbard ground station. Scientific data collected in one orbit of operations (**14 Gbit**) is stored and then downlinked in 200 s; in the meantime, also all the telemetry data (max **819 kbit**) is downlinked and all the necessary telecommands and ranging data (max **400 kbit**) is uplinked.

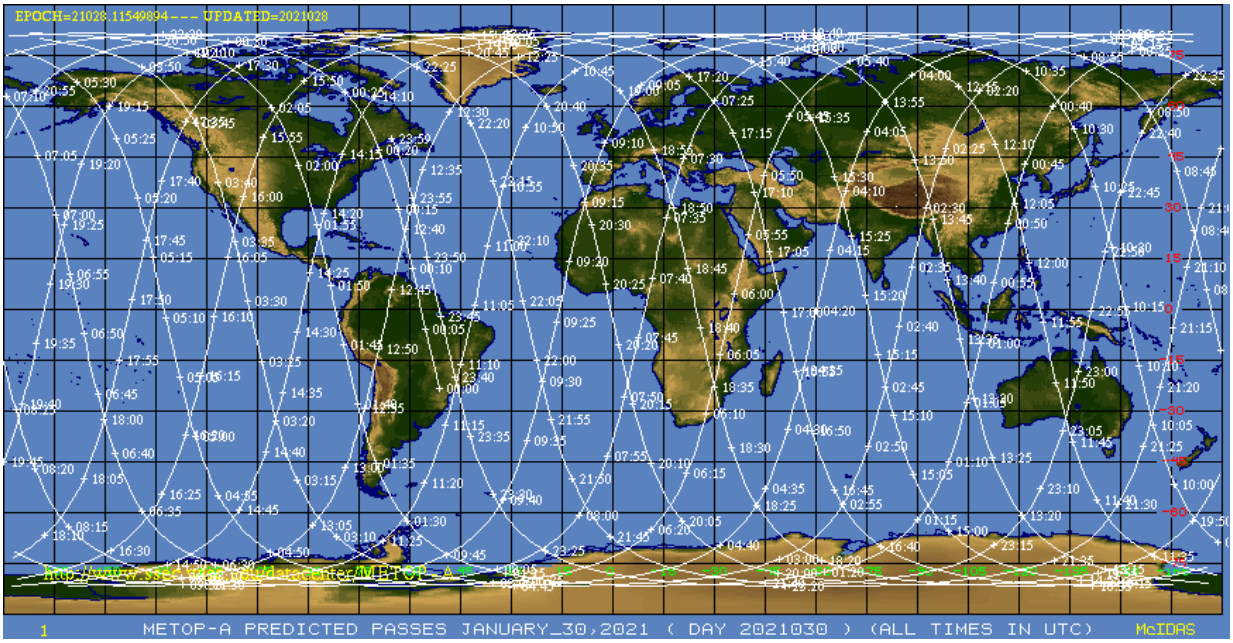

Figure 3.7: MetOp-A orbit ground tracks

3.3.7 Link budget U/D

- X-band: only downlink, **Eb/N0 = 21.46 dB**, higher than the minimum required of 8.5 dB; **SNR margin = 3.46 dB**, higher than the 3 dB minimum.
- S-Band:
    1. Downlink: **Eb/N0 = 49.08 dB**, **SNR margin = 3.73 dB**.
    2. Uplink: **Eb/N0 = 87.95 dB**, **SNR margin = 33.12 dB**.
- In both cases Eb/N0 is higher than the minimum required of 8.5 dB, and SNR margin is higher than the 3 dB minimum.

3.3.8 Positioning of the antennae in the configuration

- All the antennas are located on the face of MetOp-A that **points towards the Earth**, allowing communication with the ground stations.

4. ATTITUDE AND ORBIT CONTROL SUBSYSTEM

Change log	
§ 4.3.1	pp. 28: deeper pointing budgets and accuracy needs analysis
§ 4.3.2	pp. 30: critical analysis and comparison between attitude sensors performance and mission requirements
§ 4.3.5	pp. 31: critical analysis and comparison between attitude actuators performance and mission requirements

4.1 MetOp-A AOCS architecture and subsystem design

For AOCS control, MetOp-A utilizes a **3-axis stability control system** that is actuated through **three 40 Nms reaction wheels** and **two magnetic torquers (MAC) of 315 Am² magnetic moment**. Orbit maneuvers are controlled through **thrust impulses** provided by the propulsion subsystem. The attitude sensing is performed with two digital **Earth sensors DES** (one nominal, one for redundancy) for roll and pitch, two digital **Sun sensors DSS** (one nominal, one for redundancy) for yaw, and **four independent 2-axis gyros**. Sensing redundancy is provided by two of the 2-axis gyros as they are in cold redundancy. The goals of the AOCS are as follows [4.2]:

- automatic 3-axis control of satellite attitude,
- orbit control for needed thrust impulses,
- management of propulsion system,
- automatic 1-axis control of solar array orientation and solar array orientation in case of electric anomaly,
- providing ancillary attitude data to payload module.

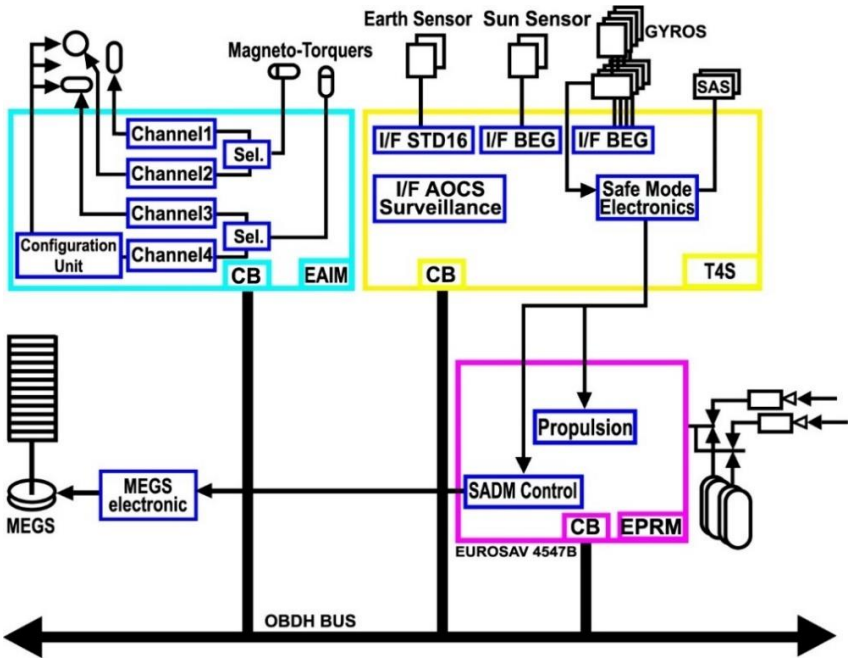

Figure 4.8: Schematic view of AOCS [4.1]

The architecture of the AOCS has three units that perform the **interface** between the SVM OBDH bus and the sensors: the EAIM, T4S, and EPRM. The **EAIM** interfaces between the reaction wheels and the magnetic torquers, the **T4S** interfaces between the Earth and Sun sensors as well as the gyros, and the **EPRM** which interfaces with the

solar-array drive mechanism as well as controls the command and acquisition capability of the propulsion subsystem [4.8].
The AOCS of the Metop-A spacecraft provides an **autonomy of 36 hours**, but it needs to be **regularly commanded from ground** in order to upload, among others, the **position within the Digital Sun Sensor** where the Sun is to be expected, to help with the control around the yaw axis, the **apparent shape of the Earth**, needed by the **Digital Earth Sensor** for accurate measurement of the pitch and roll de-pointing from the local normal direction, and the **position in the orbit** where to set the origin of the rotation of the solar panel around the spacecraft body. **Up to 72 hours of autonomy** are possible for the satellite with mission performance requirements only slightly degraded, as well as a **safe mode** that can manage performance for up to 7 days in the case of ground station issues.
Coupling of the **Sun sensor** with the **Earth sensor** provides a **complete determination** of the **orientation** of MetOp-A in space: the former provides the relative position unit vector between the spacecraft and the Sun measured in the body fixed frame to ensure attitude control in yaw, the latter computes the direction vector of the Earth with respect to the spacecraft to nearly continuously monitor the pitch and roll pointing of the platform, making it possible to construct the full attitude by combining the two measurements using, for example, the TRIAD method. The **gyroscopes** are mostly utilized on a by-request basis to provide calibration support. There are also **Sun Acquisition Sensors** that support the safe mode when necessary.
The **thrusters** of MetOp-A provide **control** for the system, specifically for **attitude pointing** due to torque imbalance created by the propulsion and coupled thrusters. The attitude control thrusters are adjusted with regards to changes in the center of mass, with one of the thrusters pulsating less than the other. The orientation of the thrusters does call for rotation around the yaw axis or a slew maneuver before an out-of-plane maneuver and an anti-slew maneuver after. A similar imbalance in the torque and thrust applies to the slew and anti-slew maneuvers as well. Throughout the maneuver phase, the attitude control thrusters are **actively controlled by the AOCS** to correct the attitude pointing due to torque imbalance created by the propulsion and coupled thrusters [4.6].

4.2 AOCS type and architecture rationale (according to control mode and pointing budget)

Control modes:

- **Orbit control** mode.
- **Sun pointed safe** mode → autonomous control through T4S survival electronics in case of ground station issues that makes it impossible to send the data needed to have the required pointing accuracy.
- **Scientific operations → high accuracy pointing**: a pointing budget of 0.07° (x-axis), 0.10° (y-axis), and 0.17° (z-axis) is required, therefore a precise 3-axis stability scheme is necessary.
- Satellite can only be **slewed** within eclipse conditions (max time for thrust is b/w 7-10.5 mins) due to instrument illumination needs.

Nominally, MetOp-A operates in **yaw-steering** and **local-normal pointing** mode, with a rotation law enabling to **compensate for the Earth rotation** velocity in the orientation

of the spacecraft and to **point the instruments** precisely in the direction of the local normal. The frame with respect to which AOCS performances are monitored and controlled is the so-called **spacecraft attitude piloting frame**. This is nominally parallel to the satellite frame, defined as a fixed reference frame with respect to the spacecraft body, but commanding capability is provided to be able to **define rotations in all three directions of the piloting frame** around the satellite frame. These rotations are uplinked in the form of the transformation matrices from the **gyroscope** axes to the desired piloting frame, for the two gyroscopes selected for attitude monitoring. It is to be noted that these rotations, contrary to the ones aiming to the correct orientation of the spacecraft prior to out-of-plane maneuvers, are carried out making use mainly of the spacecraft **reaction wheels**, and if higher torque is needed, or as a backup, of **magnetic torquers**, and **not the thrusters**. This means that, if everything works as expected, they do not imply a waste of fuel [4.7].

4.3 Reverse sizing

4.3.1 Pointing budgets inputs for AKE, APE, drift, rates

Control mode	Requirement	Solution	Type of control	Accuracy
Orbit control mode	Pointing while thrusting	3-axis stabilized	Attitude sensors, thrusters	AKE < 0.01° APE < 0.05°
Scientific operations	Local-normal pointing	3-axis stabilized	Attitude sensors and actuators	AKE < 0.01° APE < 0.05°
Power generation	Solar array optimal orientation	1-axis control of solar array	Sun sensors, solar array actuators	AKE, APE 0.1-0.5°
Sun pointed safe mode	Sun pointing	2-axis control	Gyros, SAS sensors, actuators	AKE, APE 1-5°
Slew manoeuvre	Soft slew rate to avoid damages	3-axis control	Reaction wheels (magnetorquers and thrusters as backup)	<0.5°/s

Table 4.5: MetOp-A pointing budgets [4.16]

Over a nominal stability time interval of 36 hours **Mean Knowledge Error MKE** and **Mean Performance Error MPE** remain within the optimal values of respectively 0.01° and 0.05°, thanks to data sent from Earth that optimize sensors performance. In the 36 hours autonomy period of scientific operations pointing mode after the correction data delivery from ground, **Knowledge and Performance Drift Errors** (**KDE**, **PDE**) are close to 0. Missing a data delivery leads also to higher drifts in the following 36 hours, in the order of the tenth of a degree. Because the drivers of the mission are performed mostly during the scientific operations mode, the requirement of **local-normal pointing** for the instruments requires that the control provided by the actuators is **3-axis stabilized**. However, because the primary power source is the solar array, the control and sensors required for accurate **sun pointing** are necessary for basic functioning of the satellite. MetOp-A is also sensitive to potential damages of the spacecraft impacting mission performance and therefore control to avoid these is also necessary. The combination of these requirements leads to the conclusion that to fulfill mission requirements, MetOp-A requires actuators and sensors that allows it to be **3-axis stabilized** and **3-axis controlled** at different stages of the mission.

4.3.2 Attitude sensor suite selection and sizing according to mode and pointing knowledge needs

- **Earth/Horizon sensors**: **2 Sodern STD 16** [4.9]: Operating depointing range: pitch range: ± 17 deg (Roll = 0), roll range: ± 33 deg (Pitch = 0); accuracy budget: 3σ, bias: 0.06 deg, typical noise: 0.042 deg.
- **Sun sensors (SSD)**: **2 Adcole Maryland Aerospace Digital Sun Sensors** [4.10]: number of Measurement Axes: 2 (each sensor), number of Sensors: 2 (1 each redundant side), field of View: ±32° x ±32° (each sensor), accuracy: ±0.1°, LSB Size: 0.125°.
- **Sun acquisition sensors (SAS)**: **2 Coarse Sun Sensors (CSS) from TNO** [4.11]: provide 2-axis coarse sun position information in the form of analogue voltage signals in a near hemispherical FOV, accuracy on sensor boresight better than ±1°, accuracy in central position of the FOV better than ±2°, noise equivalent angle < 0.1°, alignment better than 0.1°.
- **Gyroscopes**: **LH3Harris technologies CIRUS** [4.12]: four 2-axis Fiber Optic Gyro (FOG) sensors in a fully redundant configuration for spacecraft attitude control, Bias Stability (1s) 0.0003°/hr, Angle Random Walk (EOL) 0.000190°/√hr, Angle White Noise 0.000025 arc-sec/√Hz, Angular Rate Range > 30°/sec, Alignment Stability < 3.5 arc-sec. (long term), < 20 arc-sec (life).

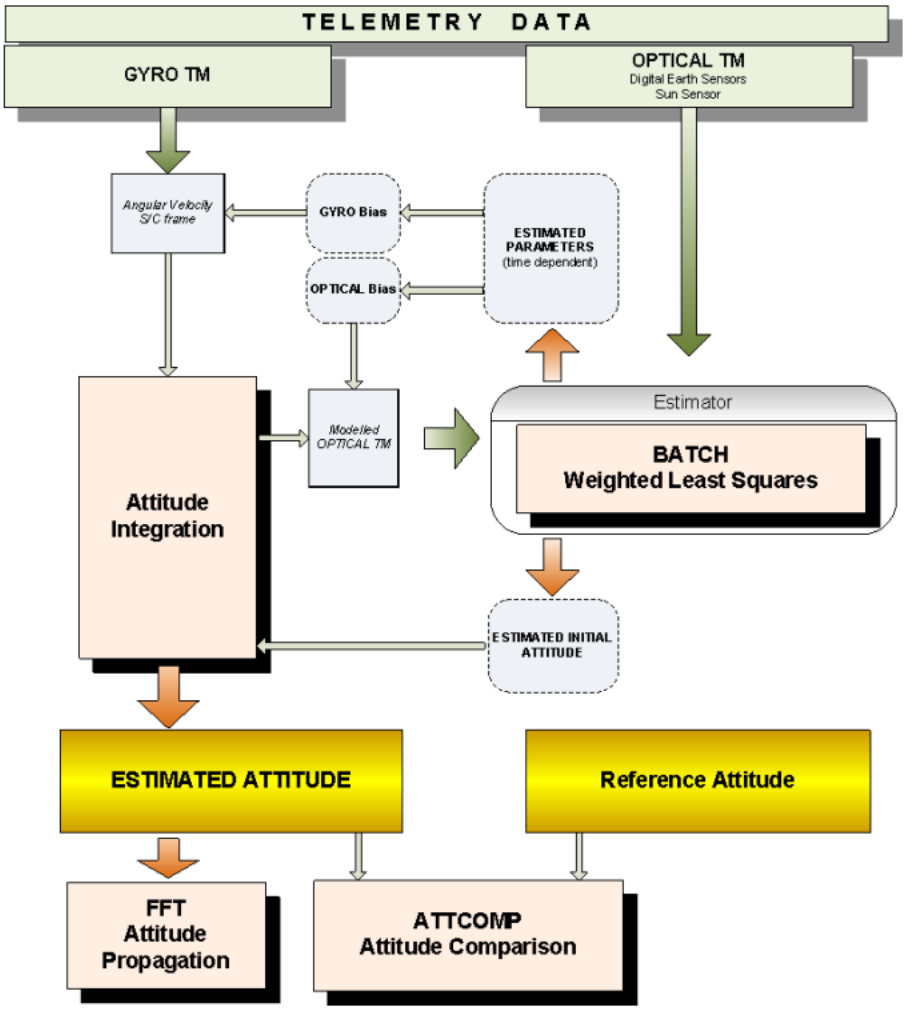

Figure 4.9: Data flow and design of the attitude determination module

The accuracy data related to these attitude sensors tells us that the **combined use of gyros**, **Earth sensors and Sun sensors** (with the help of **data sent from ground** that optimizes the sensors performance) during the **scientific operations** allows a very accurate attitude determination, giving the actuators the necessary input to **meet the accuracy needs and pointing budgets** listed in Table 4.5. The **lack of the optimization data** leads to a degradation of attitude determination performance, increasing MKE and MPE but keeping them **within acceptable values** (compliant with needed pointing accuracy of 0.07° (x-axis), 0.10° (y-axis), and 0.17° (z-axis)) for 72 hours. After this period without ground station communication, MetOp-A can't meet anymore the needed pointing requirements, and so it enters **Sun pointed safe mode** until ground communication is re-established. **Passive SASs** are used in sun pointed safe mode, with the aim of keeping the satellite alive waiting to retrieve nominal operating conditions (especially from the pointing accuracy point of view, that is the parameter most affected by the lack of data sent from ground) and to go back to scientific operations as soon as ground station communication is restored.

4.3.3 Attitude actuator suite selection according to mode

- **Reaction wheels**: **Bradford Space W18** [4.13]: 40 Nms momentum storage, 4000 RPM Maximum Operational Speed, 0.248 Nm Maximum Gross Torque, 80 ms torque rise/fall time.
- **Magnetic torquers**: **ZARM Technik AG MT400-2** [4.14]: max 400 Am^2 linear dipole moment, 750 mm length, 56 mm diameter.
- **Thrusters**: **16 MONARC 22-6** [4.15]: hydrazine monopropellant thrusters with 22.7 N nominal thrust and 230 s specific impulse; 8 main ones and 8 ones for redundancy, they provide torque around the three axes, leading to a complete rotation control, and thrust in the ±Y axis.

Reaction wheels are the main actuators of MetOp-A's AOCS: they provide torque to counteract disturbance torques (gravity gradient, solar radiation pressure, aerodynamic drag, magnetic field) and to perform slew maneuvers in **all modes**. Magnetic torquers are used for **redundancy**, as MetOp-A doesn't have a fourth reaction wheel with that purpose, and as an aid to RWs during desaturation and in emergency cases when more torque could be necessary. Thrusters are used for **orbital correction maneuvers** (especially immediately after the release of MetOp-A from the rocket's fairing), and to **desaturate** reaction wheels.

4.3.4 Disturbances effects, slew maneuvers, per mode

During its operational life the spacecraft is affected by external disturbances coming from different sources. The most relevant are **atmospheric drag**, **solar radiation pressure**, **gravity gradient** and **magnetic field**. Evaluating these contributions and adding a **safety margin of 100%** we obtain a disturbance torque value of **0.0042 Nm** (per orbit). For slew maneuvers, the worst scenario is the case in which the satellite must perform a **180°** rotation around the major axis of inertia with a maximum fixed slew rate of **0.5°/s**. In this situation **T slew = 0.2025 Nm.** In nominal condition, it is not necessary to slew the spacecraft but, in a scenario where this is needed (for example at the releasing from the carrier rocket fairing or after an emergency situation when nominal pointing must be re-established), it is possible to achieve it successfully.

4.3.5 Attitude actuator sizing according to disturbances and requested slew manoeuvres per mode with redundancy

- **Reaction wheels**: 40 Nms momentum storage, 4000 RPM Maximum Operational Speed, 0.248 Nm Maximum Gross Torque, 80 ms torque rise/fall time.
- **Magnetic torquers**: max 400 Am^2 linear dipole moment, 750 mm length, 56 mm diameter.
- **Thrusters**: hydrazine monopropellant thrusters with 22.7 N nominal thrust and 230 s specific impulse; 8 main ones and 8 ones for redundancy.

These actuators are compliant with the performance requested during the operational life but also for non-nominal pointing modes. RWs momentum storage allows them to **counteract disturbance torques** and **control the attitude** for approximately **1.5 orbits** before they saturate; thrusters are used to **desaturate** them and restore their nominal functioning: their number, configuration and nominal thrust makes it possible to desaturate the 3 RWs in less than **1 s**, but for a better accuracy and safety of the operation we impose a **desaturation time of 5 s**. In emergency situations, for example to exit from Sun pointed safe mode, **slew maneuvers** can be performed thanks to RWs (0.248 Nm Maximum Gross Torque and 4000 RPM Maximum Operational Speed allow to perform even the worst-case scenario 0.2025 Nm slew maneuver with a slew rate of 0.5°/s) with the aid of magneto torquers and thrusters if needed.

4.3.6 Fuel mass according to attitude SK, maneuvers, desaturation

Starting from previous Mission Analysis results we found that MetOp-A needs **478.9 kg** of propellant to ensure completely nominal operability during its 5 years lifetime; from the Δv preliminary analysis it was foreseen that approximately **360 kg** of propellant would have been needed for environmental disturbance forces and torques compensation. Having Reaction Wheels on board, it is necessary to de-saturate them when no further torque can be provided. Computing the value of propellant mass needed to do this operation during MetOp-A lifetime we came up with **353 kg**. As it was noticed during propulsion subsystem analysis, an higher value with respect to the fuel mass actually loaded inside MetOp-A is found because the calculations are performed using a very conservative margin of 100% for total disturbance torques (as a preliminary estimation/statistical analysis was performed) [4.3].

4.3.7 Subsystem budgets: mass, power, data

Components	N°	Mass	Power	Data
Sun sensors [4.10]	2	1.3 kg	1 W	two 10-bit data words + 1 sun presence bit
Earth sensors [4.9]	2	3.5 kg	7.5 W	1 Hz
Gyroscopes [4.12]	4	3.85 kg	10 W	-
Sun acquisition sensors [4.11]	2	0.21 kg	passive	-
Reaction wheels [4.13]	3	6.7 kg	29 W	Up to 10 Hz
Magnetic torquers [4.14]	2	11 kg	9 W	-
Thrusters [4.15]*	*16*	*0.72 kg*	*30 W*	-
Total	**-**	**67.52 kg**	**162 W**	**-**

*Table 4.6: AOCS subsystem budgets (*not included in total, as already considered part of propulsion subsystem)*

4.3.8 Positioning of the sensors and actuators in the spacecraft configuration

- **Sun sensors** and **Sun acquisition sensors**: located at the lower end of MetOp-A's face that points towards the Earth to have free field of view and positional stability; the DSS Field of View (FOV) is a slit normal to the radial direction with semi-angle of ~21 degrees and an off-pointing (with respect to the orbital velocity) of ~36 degrees toward port-board; the Sun is observed once per orbit, close to the northernmost position, (when the Sun enters into the satellite's zenith hemi-space, as in Figure 4.10), and the deviation between that observation and the expected one is used first of all to reset the yaw error to zero and then to calibrate the gyroscopes to ensure accurate yaw commanding during the entire following orbit.

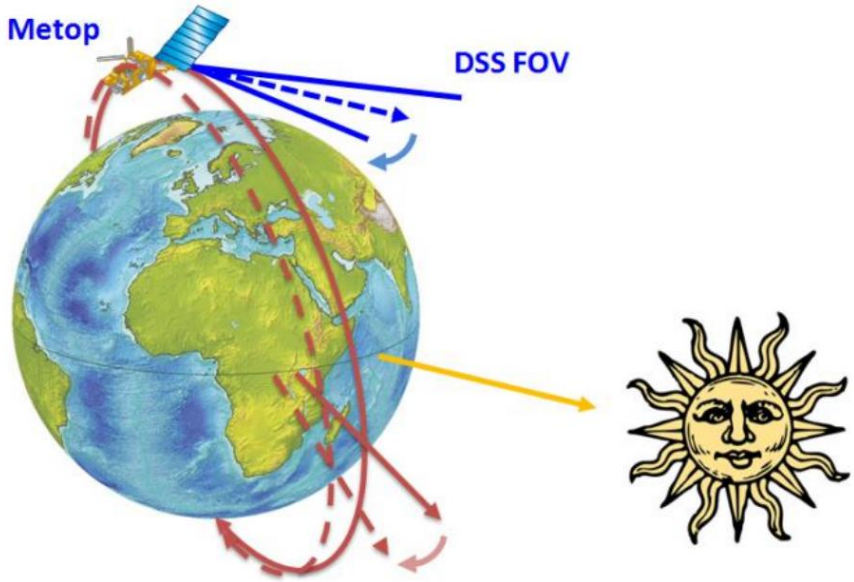

Figure 4.10: MetOp-A DSS FOV at the Sun observation time of each orbit

- **Earth sensors**: located at the lower end of MetOp-A's face that points towards the Earth, to have free field of view and positional stability; they point towards the Earth, that is -Z axis.
- **Gyroscopes**: mounted on a low vibrating part of the inside structure of the spacecraft, for better accuracy and stability.
- **Reaction wheels**: placed inside the satellite, each pointing toward one of the axes, evenly distributed so the torque is not concentrated in a critical point.
- **Magnetic torquers**: located inside the spacecraft, tied to the structure for better stability, far from electronics and OBDH to avoid magnetic interference, they provide aid and backup torque for reaction wheels.
- **Thrusters**: placed on the ±Y and ±Z outside faces of the satellite, to avoid plume impingement on the outside structure of the spacecraft and on other components located externally, and to have maximum moment arm; four of the thrusters located on the +Y face and four on the -Y face are oriented so that their combined action results in providing only thrust in + or – Y direction, without generation of torque. The orientation of all the thrusters lead to combined action of subgroups of them providing only torque (8 thrusters around Z axis, 4 ones around X axis, 4 ones around Y axis), without thrust.

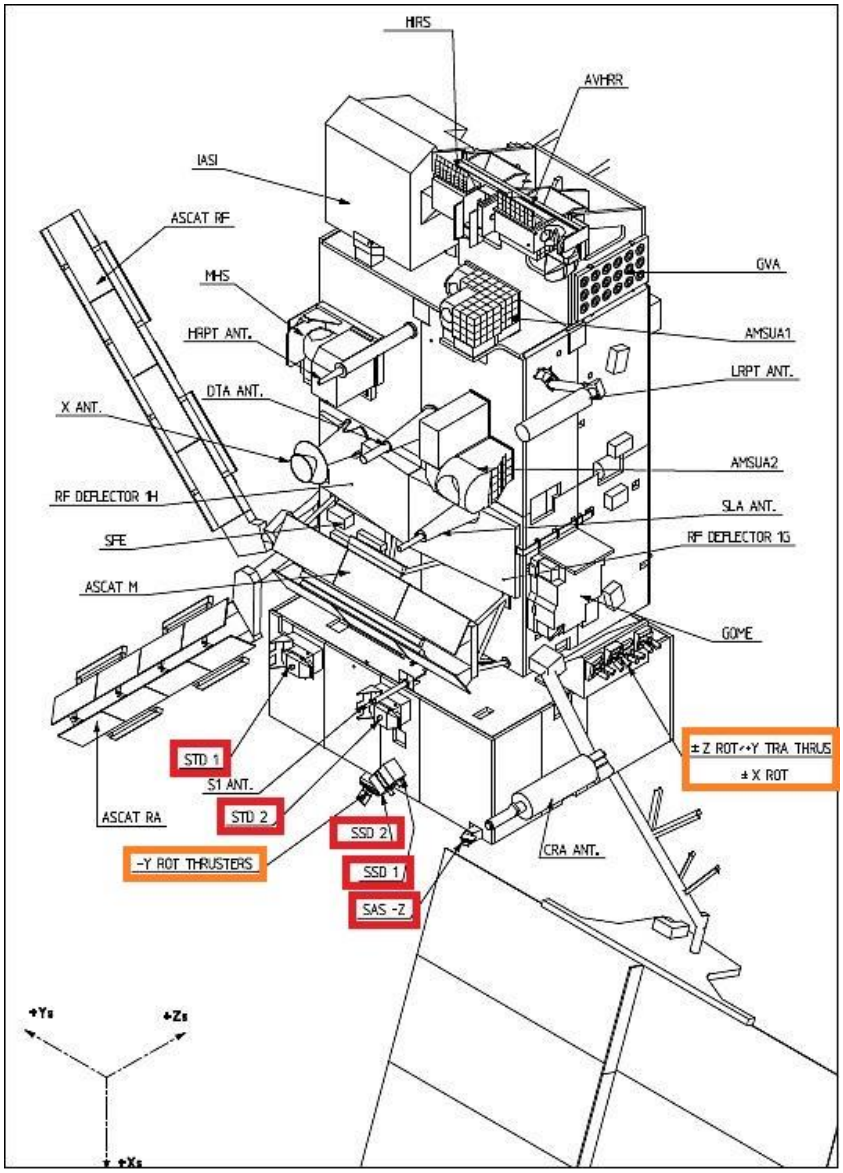

Figure 4.11: Line drawing of the MetOp-A spacecraft with part of the thrusters, Earth sensors (STD), Sun sensors (SSD) and Sun Acquisition Sensors (SAS) highlighted

5. THERMAL CONTROL SUBSYSTEM

5.1 MetOp-A TCS architecture and solutions for subsystem design

MetOp-A's thermal control subsystem architecture can be divided into two parts: **Service Module** (**SVM**) TCS and **Payload Module** (**PLM**) TCS.

5.1.1 SVM TCS

Four main areas of the Service Module [5.6] need thermal control:

- The **main body**, where all the **heat dissipating units** are installed on the side and floor panels. The **external radiators** are finished with **silvered FEP Teflon** tape. **Multi-Layer-Insulation** (MLI) blankets cover all the other faces of the main body to minimise the heat flow. Internally the panel and the electronics units are **black painted** to maximise the radiative exchanges.
- The **batteries**, directly mounted on a **radiator** plate and enclosed in a compartment **thermally insulated** from the rest of the spacecraft.
- The **propulsion equipment**, conductively **insulated** from the spacecraft; the tanks and piping are temperature controlled using **MLI** and **heaters**.
- The **solar array**, which once deployed, provides **its own thermal control** (using **passive** means such as MLI and adequate thermal finishes). Active thermal control (**heaters**) is used only during the period after the separation of the spacecraft from the launcher and up to the completion of the solar array deployment.

Figure 5.12: MetOp-A external view. Silver-coloured radiating surfaces stand on the golden-coloured MLI

5.1.2 PLM TCS

Thermal control of the PLM [5.7] is **passive** (i.e., **radiators** and **MLI**) and supplemented by **active heaters**. These are the main elements of the TCS:

- Multi-Layer-Insulation (MLI).
- flexible Secondary Surface Mirror Radiator.
- thermal doublers to spread the heat of high dissipating units.
- black paint on inner side of PLM panels.
- hardware controlled heaters.
- software controlled heaters.
- monitoring thermistors.

Hardware controlled heaters use thermostats and maintain minimum non-operating temperatures to allow immediate activation of the:

- Payload Module Computer (PMC).
- Thermal Control Unit (TCU).
- Power Distribution Unit (PDU).
- Power Control Unit (PCU).

Software controlled heaters are controlled by the PMC based on thermistor readings and defined temperature limits. They are used for warm-up and to control operational temperatures. Most instruments have **their own thermal control** and are thermally de-coupled from the PLM structure. For the Advanced Very High-Resolution Radiometer (AVHRR), High Resolution Infra-Red Sounder (HIRS) and Search and Rescue Repeater (SARR) instruments, baseplate temperatures are controlled by PLM.

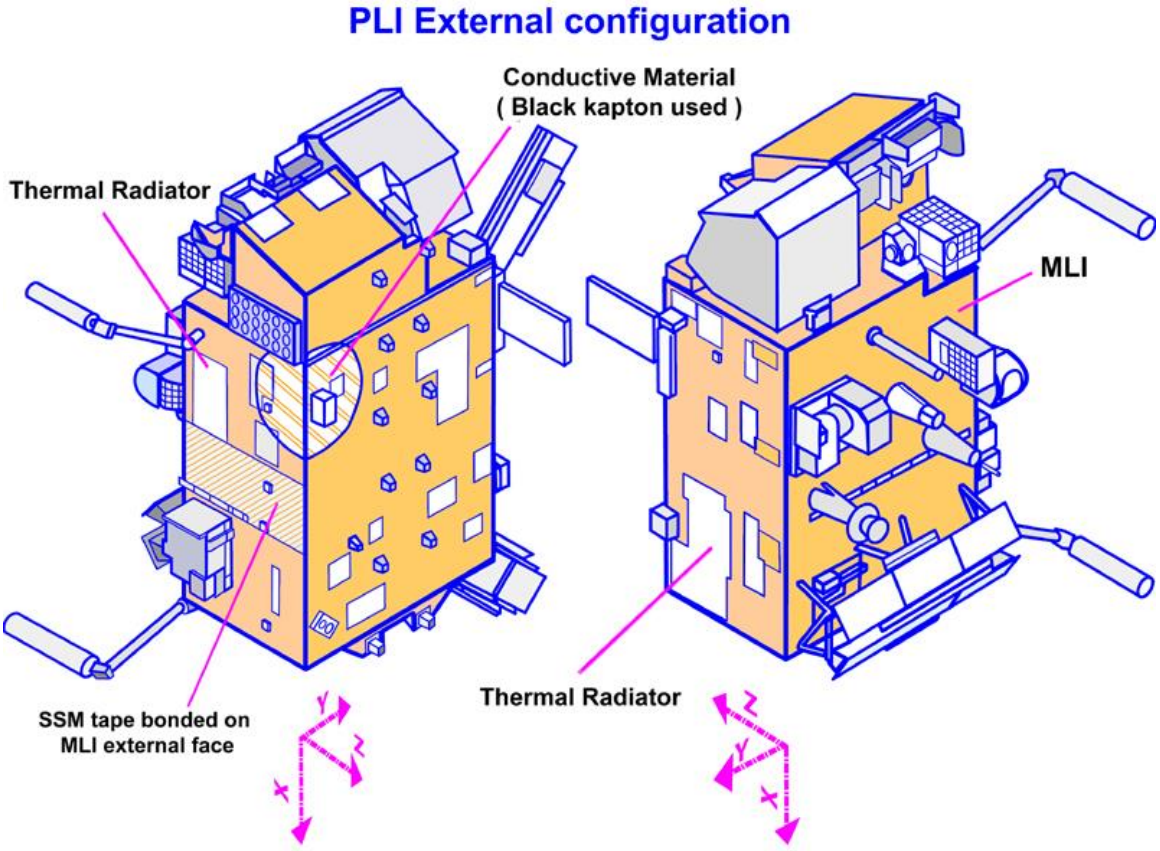

Figure 5.13: PLM external TCS configuration

5.2 TCS architecture rationale

5.2.1 External/internal thermal fluxes encountered along the mission phases

MetOp-A always encounters the same **external fluxes**, as it performs all its phases at the same Low Earth Orbit. **Maximum** and **minimum internal power generated** derive from a preliminary estimation of the spacecraft **efficiency**. This imperfect efficiency leads to the waste of a certain percentage of the electrical power generated on board in the form of thermal power emitted by active components [5.1].

Source	Maximum	Minimum
Internal power generated	2000 W	1500 W
Sun	1367.5 W/m^2	0 W/m^2
Albedo	379.5 W/m^2	351.1 W/m^2
Infrared	293.5 W/m^2	271.5 W/m^2

Table 5.7: external/internal thermal fluxes encountered along MetOp-A mission phases

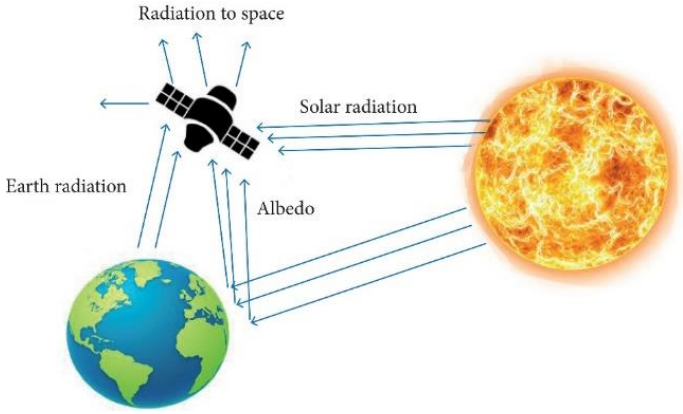

Figure 5.14: thermal fluxes for a LEO satellite

5.2.2 Requested T intervals to be respected on board

Component	Operational T range	Survival T range	Notes
Li-ion batteries [15]	-20°C – +60°C	-40°C – +60°C	Dedicated radiator and insulation
Solar panels	-150°C – +110°C	-200°C – +130°C	Dedicated TCS
Antennas	-100°C – +100°C	-120°C – +120°C	
Hydrazine tanks and lines [8]	0°C – +50°C	0°C – +50°C	Dedicated insulation and heaters
Data processing units	-20°C to +50°C	-40°C – +75°C	Dedicated thermal doublers, heaters, SSR
Earth sensors [9]	-20°C to +50°C	-40°C – +65°C	
Sun sensors [10]	-	-45°C – +85°C	
Sun Acquisition Sensors [11]	-	-80 °C – +100 °C	
Gyroscopes [12]	-23°C – +41°C	-	
Reaction Wheels [13]	-15°C – +60°C	-	
Magnetorquers [14]	-40°C – 85°C	-50°C – +125°C	

Table 5.8: MetOp-A components temperature ranges

From Table 5.8 we derive the ranges of temperature of the spacecraft to perform a mono-node analysis, that is **0°C – +41°C**; considering a preliminary analysis margin of **±15°C** [5.3] the range becomes **+15°C – +26°C**.

5.3 Reverse sizing

A **preliminary steady-state mono-node thermal analysis** is performed to verify which **material** is more suitable as external cover of MetOp-A, and to check if and for which extent **cooling** during the hot case and **heating** during the cold case are needed.

Material	Hottest T	Minimum radiators surface	Lowest T	Minimum heaters power
MLI	555 K	21.2 m^2	282 K	576 W
Aluminized Kapton	302.4 K	10.5 m^2	221.4 K	12035 W
Polished metal (Aluminium alloy)	430.9 K	35.8 m^2	243.2 K	6248 W
Al/FEP	247 K (too low)	-	-	-
Beta cloth	281.4 K (too low)	-	-	-

Table 5.9: preliminary MetOp-A mono-node thermal analysis results

This trade off leads to the choice of the **Multi-Layer Insulation** (MLI) as external cover of the satellite, considering that it doesn't require a too high **minimum radiator surface** to ensure enough cooling at the hottest point (28% of the total external surface of the spacecraft), and, at a preliminary level, it brings to the lowest **minimum heating power** needed at the coldest point (it's a too high value anyways, but it will be justified in a more refined analysis about heating power performed below).

5.3.1 Cold and hot case selection, along the whole mission

- **Cold case**: eclipse, higher distance from the Earth: apocentre of the LEO orbit (7438.9 km).
- **Hot case**: sunlight, lower distance from the Earth: pericentre of the LEO orbit (7154.8 km).

5.3.2 Adopted control strategy, passive & active

- **Passive thermal control**: MLI, external radiating surfaces, internal surfaces black painting, thermal doublers, Secondary Surface Mirror, thermal finishes.
- **Active thermal control**: thermostats, thermistors, heaters.

5.3.3 Selected materials and areas for passive control

- MLI with external **aluminized Kapton** (absorptivity α = 0.4, emissivity ε = 0.6) layer and 25 alternate internal layers of **aluminized Mylar** (absorptivity α = 0.12, emissivity ε = 0.03) and **Dacronor silk net**: effective MLI absorptivity α = 0.004, effective MLI emissivity ε = 0.02 [5.16][5.17][5.18], **Area = 54.3 m^2**.

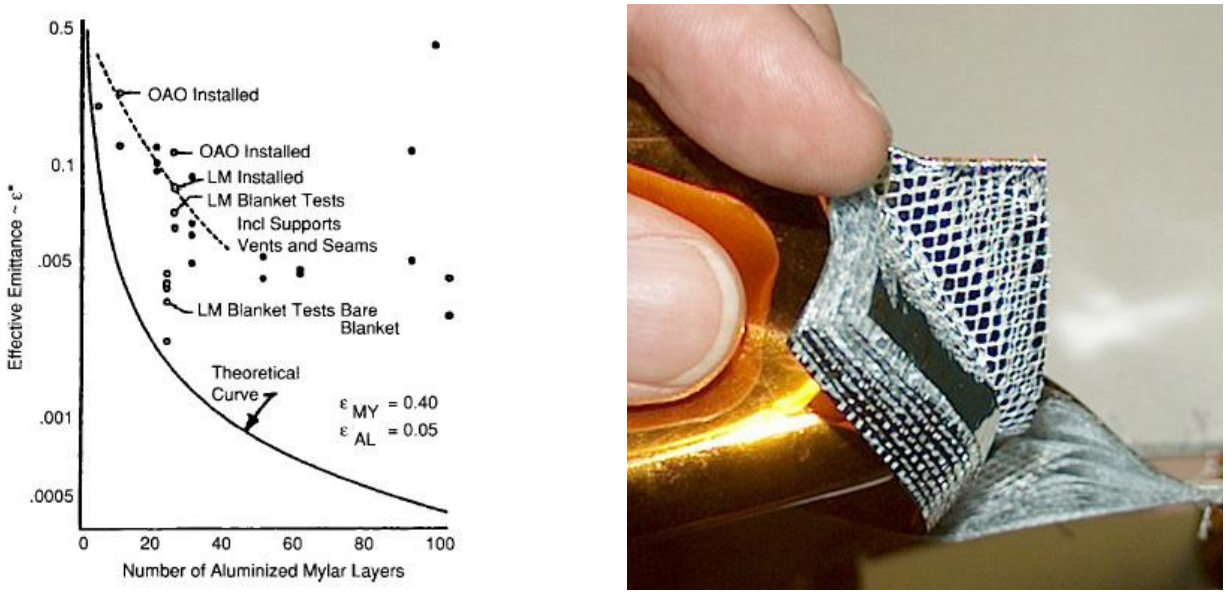

Figure 5.15: MLI effective emittance and internal structure

- External radiators finished with **silvered Teflon** (absorptivity α = 0.09, emissivity ε = 0.8) [5.4][5.5], **Area = 21.2 m²**.
- **Black Kapton** thermal doublers, **Area ≈ 0.5 m²**.
- **Silver coated FEP** (absorptivity α = 0.09, EOL absorptivity α = 0.3, emissivity ε = 0.78) Secondary Surface Mirror [5.4][5.5]; the SSM substitutes a radiating surface for a portion of the spacecraft that needs lower entry flux and higher emission, **Area ≈ 0.5 m²**.

5.3.3 Needed electric power for active control

In the **cold case** the spacecraft lowest temperature is about **281 K**, which is lower than the minimum one it can withstand, assumed to be **288 K**. In order to stay within this range, heaters are needed. The power required to heat the whole spacecraft is **576 W**. This is a too high value, consisting of more than one fourth of the total power MetOp-A consumes over one orbit. It's important to notice that not all the components of the satellite need heating: as shown in Table 5.8, many of them can withstand even the calculated margined lowest temperature the spacecraft reaches. For this reason, it is possible to save power by **applying heaters just to the most low-temperature-sensible components**, listed in the following section.

5.3.4 Units specifically controlled

Heaters maintain minimum non-operating temperatures of **propulsion equipment** (4 for the tanks, 3 for the feeding lines), **solar array** (only during the period after the separation of the spacecraft from the launcher and up to the completion of its deployment), **Payload Module Computer** (PMC), **Thermal Control Unit** (TCU), **Power Distribution Unit** (PDU), **Power Control Unit** (PCU), and operating temperatures of the most low-temperature-sensitive scientific instruments and components.

5.3.5 Subsystem budgets: mass, power, data

Components	N°/Area	Mass	Power	Data
MLI	54.3 m^2	43.44 kg (0.8 kg/m^2 [5.23])	passive	-
Radiators	21.2 m^2	7.87 kg (0.371 kg/m^2 [5.24])	passive	-
Thermal doublers	≈ 0.5 m^2	36 g (72 g/m^2 [5.25])	passive	-
Secondary Surface Mirror	≈ 0.5 m^2	273 g (546 g/m^2 [5.26])	passive	-
Heaters	15	≈ 6 g (0.04 g/cm^2 [5.27]	≈ 75 W [5.27]	≈ 7.5 KIPS, 4 kb ROM, 11.5 kb RAM [5.28]
Total	**-**	**≈ 51.625 kg**	**≈ 75 W**	**≈ 7.5 KIPS, 4 kb ROM, 11.5 kb RAM**

Table 5.10: TCS budgets

5.3.5 Positioning of the control components in the s/c configuration

- The **Multi-Layer-Insulation** (MLI) blankets cover all the faces of the main body.
- **External radiating surfaces** are located in correspondence of components that generate a lot of thermal power and need to dissipate it to not overheat (batteries, on board computer, electronics and some scientific instruments).
- Internally the panels and the electronics units are **black painted** to maximise the radiative exchanges.
- **Thermal doublers** spread the heat of PLM computer and distribution and control units.
- A **flexible Secondary Surface Mirror Radiator** is bonded on a subsection of PLM MLI -Y external face to limit the entry flux while maximising the emission in correspondence of components that need extra heat emission.
- **Heaters**, **thermistors** and **thermostats** are attached to the aforementioned components and instruments whose temperature need to be controlled and that need to be warmed up not to reach too low temperatures.

5.3.6 Imposed specific pointing direction for any passive control surface

Passive control surfaces are placed on **all the external surfaces** of the spacecraft **apart from the Earth-pointing one** (-Z), to dissipate heat better towards deep space.

6. ELECTRIC POWER SUBSYSTEM

Change log	
§ 6.2.1	pp. 42: Table 6.11 revised with power required per phase/mode of the mission
§ 6.3.1	pp. 43: link to Table 6.11 for power required per subsystem per phase/mode
§ 6.3.6	pp. 45: Table 6.14 revised with power budget per phase/mode of the mission

6.1 MetOp-A EPS architecture and subsystem design

On MetOp-A electrical power is generated by an **eight-panel solar array** (SA) derived from the Environment Satellite (ENVISAT). It has a **single wing**, **flat pack** design solar array. It consists of **eight hinged rigid solar cell panels** (each 1 m x 5 m), equipped with **BSR type solar cells**. The solar array cant angle is 20° and the generated power capability is **3828 W end of life**. The satellite commands and monitors solar array deployment keeping track of:

- deployment progress,
- position indicators,
- temperature of the deployment motors and panels.

The array electrical power is transferred through a cable harness along the **primary deployment arm** up to the **Solar Array Drive Mechanism** (**SADM**), mounted on the spacecraft side of the interface. The SADM rotates to hold the solar array correctly orientated towards the Sun.

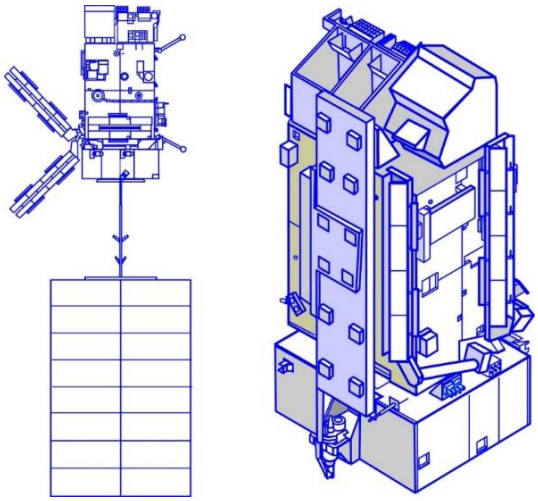

Figure 6.16: Solar array deployed and stowed configuration

Five batteries store energy, allowing power supply during:

- Launch and Early Orbit Phase (LEOP),
- eclipse and contingency mode,
- temporary power peak demand above the solar array capability during sunlight.

The **primary power bus** is **unregulated** and distributes power to the Service Module (SVM) and Payload Module (PLM) units. The 28 V power regulation needed by the American instruments is provided by a dedicated Power Control Unit (PCU) located in the PLM. Power is controlled by a dedicated unit (RSJD) that is in charge of the:

- balance among the power provided by the solar array,
- spacecraft power demand and the batteries recharge,
- distribution of several power buses,

- managing the batteries' thermal control,
- provides switch-off lines for the satellite management in case of failure conditions [6.6].

6.1.1 Service module power buses

- Permanent **22-39 V unregulated** power buses: BNR/PF for all the SVM functions in nominal and safe modes, except EAIM (using BNR/EAIM) and SVM thermal control heaters (using BNR/CH/PF). BNR/CU 1 and 2 for PLM avionics and services. BNR/CH/CU for PLM and European Instruments thermal control.
- Permanent **50 V regulated** power bus (BRP) for SVM low-level electronic functions and bus couplers (for both SVM and PLM) in nominal and safe modes, as well as for the Payload Module Controller (PMC).
- Switched **50 V regulated** power buses (BRA 1 and 2) derived from BRP, used for switching of SVM and PMC bus couplers.
- The **RSJD** provides **several power buses**, and switch-off lines for the satellite management under failure conditions. The PLM power distribution is ensured by the PDU, which provides lines protected by latching current limiters [6.7].

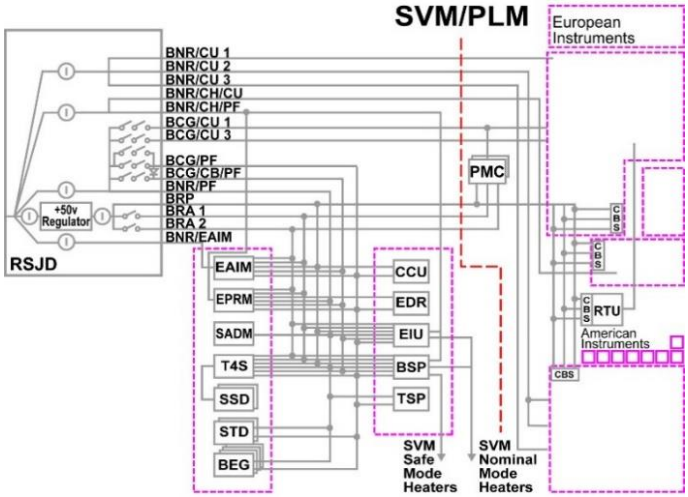

Figure 6.17: RSJD power distribution

6.1.2 Payload Module electrical power distribution, control and harness

The following elements are involved: Power Distribution Unit (PDU), Power Control Unit (PCU), Thermal Control Unit (TCU), PLM Interpanel and Panel Harnesses.
The Power Distribution Unit (PDU) uses power from the Service Module (SVM) to supply **unregulated** power (**22 – 37.5 V**) to all PLM equipment and European instruments. To provide switching and protection functions, the PDU uses Latch Current Limiters (LCL). The PDU also supplies power for the motor driven deployment of the Advanced Scatterometer (ASCAT) instrument, Low Resolution Picture Transmission (LRPT) and Combined Receive Antenna (CRA) antennas. The Power Control Unit (PCU) provides **regulated** power to the National Oceanic and Atmospheric Administration (NOAA) instruments at **28 V**. A Thermal Control Unit (TCU) is dedicated to supplying **unregulated** power to the heater mats. Various types of **harness**:

- panel harness located on each structure panel,
- inter-panel harness connecting panels to panels and external elements,
- instrument harness connecting the various elements within an instrument.

Connector brackets on the panels make it easy to attach the harnesses and re-assemble the PLM elements after integration and testing. Interface connectors are used for harnesses that run from the inside to the outside of the PLM. For power and signal harnesses, purpose-built clamp shells are used [6.8].

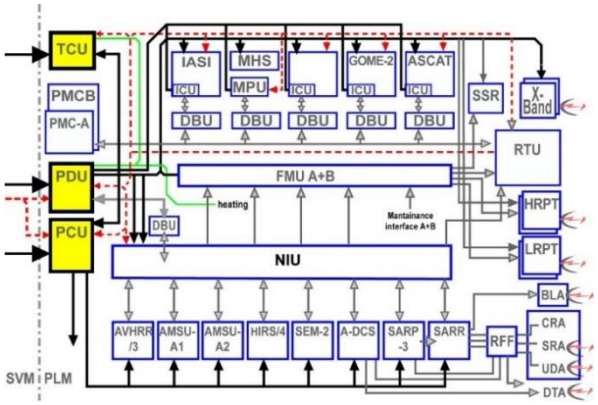

Figure 6.18: Metop-A's power distribution within the payload module

6.2 EPS architecture rationale

6.2.1 Electric Power and Energy requested in each mission phase

MetOp-A performs all its phases in the same LEO, and all the instruments work in the same way (and so require the same power) both in **daylight** and during **eclipse time**; To perform the reverse sizing, it was considered a worst-case scenario in which MetOp-A spends one third of each orbit (**34 minutes**) **in eclipse**, and the remaining **67 minutes in daylight**. There is a slight difference in the requested power between daylight and eclipse time: during the former the mechanisms and components that drive the solar array functioning and its power distribution are switched on while the heaters are switched off, during the latter the opposite happens; moreover, the satellite has a relatively small peak power during the 200 s communication window when TTMTC needs 120 W to send scientific data and telemetry to the ground station. The highest **power demand** (1.81 kW) is considered for the preliminary analysis.

Subsystems	**Power needed**		
	daylight	**eclipse**	**communication**
Instruments	885 W	885 W	885 W
PLM (OBDH, TTMTC, TCS, EPS)	371 W	371 W	491 W
SVM (PS, ADCS, TCS, EPS, OBDH)	387 W	387 W	387 W
Solar array	50 W	-	50 W
Heaters	-	75 W	-
Total	**1.69 kW**	**1.72 kW**	**1.81 kW**

Table 6.11: MetOp-A required electric power [6.1]

6.2.2 Operational profiles and available sources

The main available power source for a satellite in LEO like MetOp-A is the **Sun**. Considering the altitude of the satellite negligible with respect to the Sun-Earth distance, the distance between the Sun and the spacecraft can be considered equal to 1 AU (150 million km); average annual **solar irradiance** arriving at the top of the Earth's

atmosphere is roughly **1361 W/m²**. For a satellite orbiting around the Earth, it must be taken into consideration that the planet's **axis is tilted** towards the ecliptic of the **Sun** at approximately **23.44°**; for the reverse sizing, it was considered a worst-case scenario **inclination angle** of the solar array with respect to the Sun of **30°**.

6.3 Reverse sizing

6.3.1 Power budget supplied per phase/mode per subsystem

Power budget supplied per subsystem per phase/mode is summarized in Table 6.11.

6.3.2 Primary source selection and sizing

Due to their low efficiency, high cost, volume and mass, issues correlated with radiations and difficulty to reach MetOp-A's high power demand, **RTGs** aren't considered as a candidate primary source. So, chosen **solar power** as primary source, a trade-off is performed between **Silicon** and **Triple Junction InGaP/GaAs/Ge solar cells**.

Parameter	Si [6.8][6.9]	InGaP/GaAs/Ge [6.10]
BOL efficiency	14.5%	29.5%
Degradation/year	2.8%	3.75%
Average weight	320 g/m²	890 g/m²
Cell area	64 cm²	30.15 cm²
Cell voltage	0.628 V	2.61 V
Max power required	**3793 W**	
Cells in series	**45**	**11**
Number of cells	**5715**	**6259**
Solar cells area	**36.576 m²**	**18.871 m²**
Solar cells mass	**11.704 kg**	**16.795 kg**
EOL power	**3796.491 W**	**3794.065 W**
Price	**1365.48 $** (0.36 $ per W [6.11])	**188710 $** (10000 $ per m² [6.12])

Table 6.12: solar cells material trade-off

The **power requested to the solar array** at **maximum power demand condition** (in daylight to feed subsystems and instruments and contemporarily charge the batteries) depends on daylight and eclipse max power requirements, daylight and eclipse times and line efficiencies, so it's the same for both the materials, and it's compliant with the actual MetOp-A solar array power capability of 3828 W end of life. Less BOL efficiency leads to a **higher area** needed for Si solar cells, while higher average weight leads to a **higher mass** of Triple Junction ones. The parameter that brings to the **final choice of Si solar cells** is the **price**: more than 138 times **lower** with respect to the Triple Junction ones. Moreover, especially when MetOp-A was launched, Si solar cells were a **less complicated** and **more flight proven** and **reliable** technology: e.g., ISS and ENVISAT used it, and MetOp-A employs the same solar array architecture as ENVISAT. Actual MetOp-A solar array **area** and **power capability** are a bit higher with respect to the calculated ones as the employed architecture implies using **1 m x 5 m** solar cell panels, leading to an oversized **40 m²** area (**8 panels**) and a slightly higher power generation. The actual **mass** of the solar array, **255 kg**, includes solar cells, structure, MLI, heaters, mechanisms, harness and primary source power control and distribution components.

6.3.3 Secondary source selection and sizing

Secondary batteries are needed to make MetOp-A's instruments and subsystems work during eclipse time, to provide electric power in LEOP before solar array deployment and in case of temporary power peak demand above the solar array capability during sunlight; a trade-off is performed between **Li-ion** and **Ni-Cd batteries**.

Parameter	Li-ion [6.4][6.5]	Ni-Cd [6.4][6.5]
Number of batteries	5	
Battery capacity	40 Ah	
Depth Of Discharge DOD (5 years in LEO, see Figure 6.19)	25% (Li-ion target for LEO)	20%
Specific energy	140 Wh/kg	40 Wh/kg
Energy density	250 Wh/dm^3	90 Wh/dm^3
Cell voltage	3.6 V	1.35 V
Required capacity	**2051.333 Wh**	**2564.167 Wh**
Battery mass	**14.652 kg**	**64.104 kg**
Battery volume	**8.205 dm^3**	**28.491 dm^3**
Cells in series	**8**	**21**
Strings in parallel	**3**	**3**
Actual battery system capacity	**2764.8 Wh**	**2721.6 Wh**

Table 6.13: secondary batteries materials trade-off

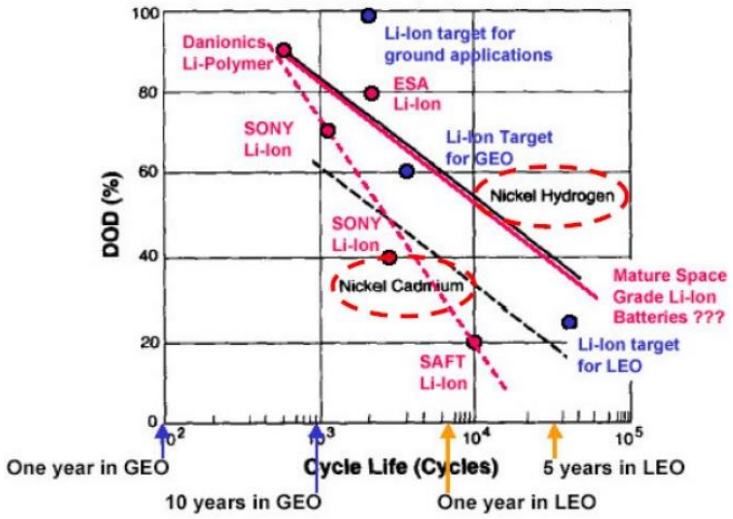

Figure 6.19: different types of secondary batteries DOD vs number of cycles

Higher DOD, specific energy and energy density make the Li-ion batteries better than Ni-Cd ones from all points of view. MetOp-A employs **5 Li-ion** batteries with **24 cells** each and a total mass of **73.262 kg**, volume of **41.027 dm^3**, and capacity of **13824 Wh**.

6.3.4 Primary source regulation adopted strategy

The **primary power bus** is **unregulated** and distributes power to SVM and PLM units. For MetOp-A **Peak Power Tracking** (**PPT**) is chosen over **Direct Energy Transfer** (**DET**) because it's more well suited for a mission with a **high number of daylight-eclipse cycles** and with many **different power buses** with **different voltages** that need to be **independent** from the solar array one; the drawbacks of being heavier, more expensive

and less efficient (PPT X_d = 0.8, X_e = 0.6) are taken into account for the trade-off but they're given a lower weight with respect to the aforementioned advantages.

6.3.5 Bus regulation adopted strategy

Many different power buses are used for the many active components and instruments of MetOp-A, summarized in these sections: SVM, PLM. **Unregulated** power buses are used for components and instruments that can work in a range of voltages, to keep them simple, cheap and light; **regulated** buses are employed for components and instruments that work at a determined and precise voltage, to ensure high flexibility, no lock-up and no transient on the bus at the price of higher weight and power losses.

6.3.6 Subsystem budgets: mass, power, volume, data

Components	Mass	Power			Volume	Data [6.13]
		sunlight	eclipse	comm.		
Solar cells	11.704 kg	-	-	-	0.0064 m^3	-
SA structure, TCS, SADM, harness, power distribution	243.296 kg	50 W + ≈ 1.7 kW losses	-	50 W + ≈ 1.8 kW losses	≈ 0.5 m^3	≈ 0.5 KIPS, 2.4 kb ROM, 3.4 kb RAM
Batteries	73.262 kg	-	≈ 2.7 kW losses	-	0.041 m^3	-
Power buses, cabling, harness	58 kg (15% of total mass [6.3])	≈ 100 W losses			≈ 0.1 m^3	≈ 4.5 KIPS, 21.6 kb ROM, 30.6 kb RAM
Total	**386.262 kg**	**50 W + ≈ 1.8 kW losses**	**≈ 2.8 kW losses**	**50 W + ≈ 1.9 kW losses**	**≈ 0.6474 m^3**	**≈ 5 KIPS, 24 kb ROM, 34 kb RAM**

Table 6.14: EPS budgets

6.3.7 Positioning of the control components in the s/c configuration: PV arrays/wings, battery packages, RTGs

- As shown in Figure 6.16, in launch configuration the **solar array** is stowed attached to the +Z face. After the deployment, the array hangs out from the +X face and it's attached to the Service Module through the primary deployment arm, that keeps it at approximately 5 meters from the spacecraft. In this way there is no risk that the array shadows the line of sight of MetOp-A's instruments, antennas and sensors, the thrusters' plume doesn't impinge on the solar cells, and the body of the spacecraft doesn't shadow the SA from the Sun.
- The **battery package** is located in the Service Module, directly mounted on a deep-space-pointing radiator plate and enclosed in a compartment which is thermally insulated from the rest of the spacecraft.

6.3.8 Specific pointing direction requirements

The **solar array Sun-pointing** is ensured by the spacecraft 3-axis stabilization and a 1-axis control of the array itself through the Solar Array Drive Mechanism (SADM).

7. CONFIGURATION AND ON-BOARD DATA HANDLING

7.1 MetOp-A space segment configuration

MetOp-A design is based on a **modular concept**. The satellite consists of a **Solar Array** and two modules: the **Service Module** (SVM) and the **Payload Module** (PLM).

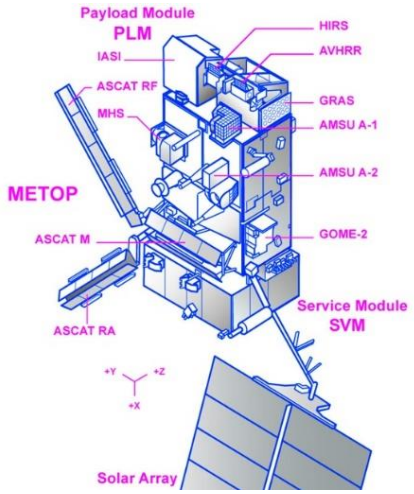

Figure 7.20: MetOp-A satellite in orbit configuration

7.2 Reverse sizing

7.2.1 Overall vehicle shape and appendages distribution according to their operational needs and technical requirements

The **S/C overall size** is: **6.2 m x 2.5 m x 2.5 m** (**launch** configuration) and **17.6 m x 6.6 m x 5.0 m** (**on-orbit** configuration). The **appendages** that, stowed in launch configuration and deployed on orbit, increase MetOp-A's size, are:

- The **solar array** hangs out from the +X face and it's attached to the SVM through the primary deployment arm, that keeps it at approximately 5 meters from the spacecraft. In this way there is no risk that the array shadows the line of sight of instruments, antennas and sensors, the thrusters' plume doesn't impinge on the solar cells, and the body of the spacecraft doesn't shadow the SA from the Sun. Its release is controlled by the Solar Array Drive Mechanism (SADM) [7.3][7.4].
- **ASCAT** needs 3 **antennas** for each of the 2 swaths; all 6 antennas are 2.5 m long slotted waveguide Al arrays; one antenna in each set looks sideward at 90°, one forward at 45°, and one aftward at 135°. 2 of them are attached to PLM -Z face, oriented at 0° with respect to Y axis, the other ones are at +45° and -45°, hanging out from +Y face. They have a clear line of sight towards the Earth, and they don't shadow other instruments, antennas and sensors [7.1]. They are released by pyros from the SVM and deployed under motor control from the PLM [7.3].
- **Low Resolution Picture Transmission (LRPT) antenna** and **Combined Receive Antenna (uplink) (CRA) antenna** hang from PLM -Y face to have a clear line of sight towards the Earth and not to shadow other instruments. they are released by the SVM and further deployed under motor control from the PLM [7.3].
- the **GPS-based Atmospheric Sounder (GRAS) GAVA antenna** hangs from PLM +Z face to allow instrument scientific operations; it is deployed by a spring mechanism which is released fully under SVM control [7.3].

7.2.2 Launcher interface location and features and vehicle configuration when in the launcher fairing

In launch configuration the **solar array** is stowed attached to +Z face (hidden in Figure 7.21), **ASCAT antennas** and **GRAS GAVA antenna** are stowed on +Y face, **LRPT** and **CRA antennas** are stowed on -Y face. The **base of the SVM** interfaces with the launcher via a **standard 1666 adaptor** via a **clamp and attachment/release device** [7.2][7.7].

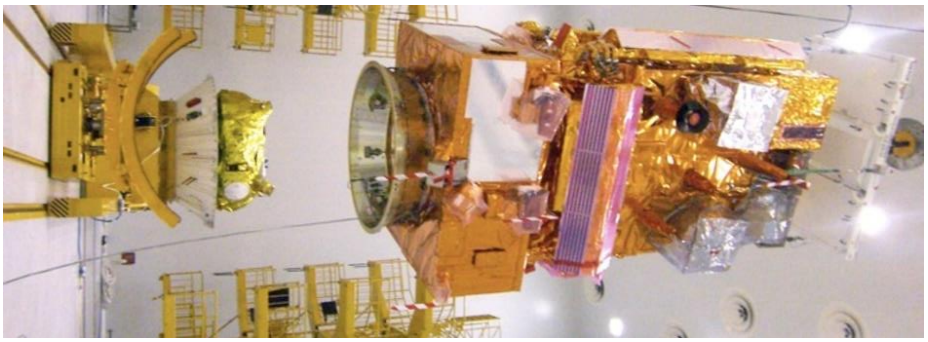

Figure 7.21: MetOp-A in launch configuration, being integrated with Fregat upper-stage 1666 adaptor

7.2.3 Distribution of the elements on the external surface: location, distance/proximity with other components, direction of the FOV, pointing needs, shadowing, etc. according to their operational requisites and constraints

On the external surface of **SVM** there are:

- **Sun sensors** and **Sun acquisition sensors**: located at the lower end of MetOp-A's Earth-pointing face to have free field of view and stability; the DSS Field of View (FOV) is a slit normal to the radial direction with semi-angle of ~21° and an off-pointing (with respect to the orbital velocity) of ~36° toward port-board.
- **Earth sensors**: located at the lower end of MetOp-A's Earth-pointing face, to have free field of view and stability; they point towards the Earth, that is -Z axis.
- **Thrusters**: placed on the ±Y and ±Z outside faces of the satellite, to avoid plume impingement on the outside structure of the spacecraft and on other components located externally, and to have maximum moment arm.

On the external surface of **PLM** there are **instrument sensors** and **antennas** and **TTMTC antennas**; most of them are mounted on -Z face and point towards the Earth (-Z direction), as shown in Figure 7.20. As stated above, some antennas are deployed outside of the S/C main body not to shadow other sensors and antennas. The **Multi-Layer-Insulation** (**MLI**) **blankets** cover all the faces of the main body; **external radiating surfaces** and an **SSM** are in correspondence of components that generate a lot of thermal power and need to dissipate it, on the external surfaces of SVM and PLM, pointing towards deep space. The external configuration of the satellite is driven by:

- the **FOV** and **performances** of instruments, sensors, radiators and antennas,
- the **available volume** under Soyuz-ST Fregat fairing (3.8 m diameter, 7.5 m height [7.11]),
- the **ease** and **cost** of manufacturing, integrating and testing,
- the **maximum de-coupling** among the various elements,
- the **accessibility** to some critical areas (e.g., where required for functional checks of instruments or sensors) [7.2].

7.2.4 Distribution/location of the internal elements with respect to their functionality and operational requisites and constraints: Centre of Mass (CoM) balancing, thermal dissipation

The **SVM** is a 'box' shaped structure that comprises the following:

- **Central structure**: made of a Carbon Fibre Reinforced Plastic (CFRP) sandwich construction cone with bonded aluminium alloy upper and lower rings.
- **Propulsion module ring**: a machined aluminium alloy plate, used to support the four **propellant tanks** and to interface with both the PLM and the SVM central structure. It's located inside the central structure to maintain the CoM as central as possible as tanks with fuel are the heaviest part of the satellite, and to keep CoM position as constant as possible considering fuel consumption.
- **Box structure**: Around the CFRP cone are Al alloy sandwich upper and lower floors and external walls, forming a rectangle with shear walls that link the central cone to the external rectangular box structure. **Gyros**, **Reaction Wheels** and **Magnetic Torquers** are attached to these panels for better accuracy and stability; RWs are evenly distributed so the torque is not concentrated in a critical point, MTs are far from electronics to avoid magnetic interference.
- **Battery compartment** includes the assembly of the battery support plate and five equi-spaced radial stiffeners; it has a deep-space-pointing radiator plate and allows thermal insulation from the rest of the spacecraft.

In the SVM there are **electronics** for power distribution, TTMTC, evenly distributed to optimize CoM balancing and thermal dissipation [7.4][7.5]. **PLM** internal structure consists of a 'box' with a central cylinder as the main structural load path to SVM, shear walls, floors, panels with thermal doublers, balcony with support webs, instrument support interface brackets and harness connector brackets. The accommodation of **instruments** is a significant design driver, and the PLM also houses **avionics** for **power regulation** and **distribution**, **command** and **control**, and **handling** and **transmission** of scientific **data**. PLM internal configuration is driven by the following principles:

- provision of **sufficient radiator area** for heat dissipation of internal units,
- **modular grouping** of PLM subsystems or functional units and instrument units to allow for pre-integration and testing on single panels,
- **minimal failure propagation** to other instruments/subsystems in case of unsuccessful antenna deployment,
- **optimal length** for loss-sensitive cabling like antenna-receiver connections,
- **optimal harness routing** conjunct with **modular assembly flexibility** [7.6][7.3].

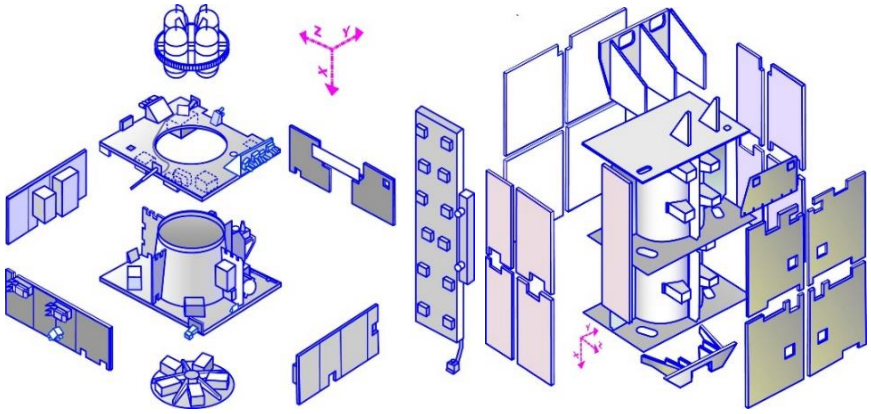

Figure 7.22: SVM internal exploded view with main subsystems (left), PLM internal structural elements (right)

7.3 MetOp-A OBDH subsystem design and architecture

MetOp-A data handling architecture considered as a whole is **decentralised**, as the **Payload Module** (PLM) and **Service Module** (SVM) have their own computers. **Standard On-Board Data Handling** (OBDH) **data buses** are used for **data exchanges** between the Service Module and Payload Module computers and the remote unit. The bus couplers are used in several SVM units to interface with the OBDH bus.

7.3.1 Service Module OBDH

The SVM data management has a **distributed bus** architecture, and it's controlled by the **Central Communication Unit** (**CCU**), including a **MA 31750 microprocessor** with **two redundant memory modules of 224 Kwords**. The CCU performs the data exchange with the OBDH bus, bus couplers and on-board time generation and synchronization. The **decoding and reconfiguration unit** (**EDR**) interfaces with the S-band transponder. It carries out:

- telecommand receipt,
- execution of Command Pulse Direct Unit (CPDU) telecommands,
- CCU supervision.

The **housekeeping and pyrotechnics unit** (**BSP**) is in charge of:

- the generation of pyrotechnics commands,
- temperature measurements,
- actuation of heaters for the SVM,
- housekeeping of some SVM units.

The **Electrical Interface Unit** (**EIU**) is responsible for the:

- release and deployment of the solar array,
- telemetry/telecommands (TM/TC) for some parts of the SVM [7.12].

7.3.2 Payload Module OBDH

PLM OBDH subsystem has a **distributed bus** architecture too; it comprises several components: **Payload Module Computer** (**PMC**), **Standard Bus Couplers** (**CBSs**), **Remote Terminal Unit** (**RTU**), **Digital Bus Units** (**DBUs**), **Standard Remote Bus Interface ASICs** (**RBIs**), **Intelligent Control Units** (**ICUs**).
The PMC controls all PLM equipment and instruments via an **ESA standard On Board Data Handling** (**OBDH**) **bus**. PLM equipment is controlled via:

- non-intelligent CBSs for power units,
- an RTU for control of the other PLM equipment,
- Intelligent Control Units (ICUs) for de-centralised instrument control.

To safeguard a common hardware interface to the OBDH bus, standard DBUs are used, and are equipped with standard Remote Bus Interface (RBI) chips inside the various ICUs. For the National Oceanic and Atmospheric Administration (NOAA) instruments a **dedicated NOAA Interface Unit** (**NIU**) and for the Microwave Humidity Sounder (MHS) a **MHS Protocol Unit** (**MPU**) have been introduced to adapt the dedicated instrument interfaces to the OBDH standard and to provide the ICU functionality. These units also adapt the respective instruments measurement data interface to the ESA standard and are therefore also part of the measurement data chain [7.13].

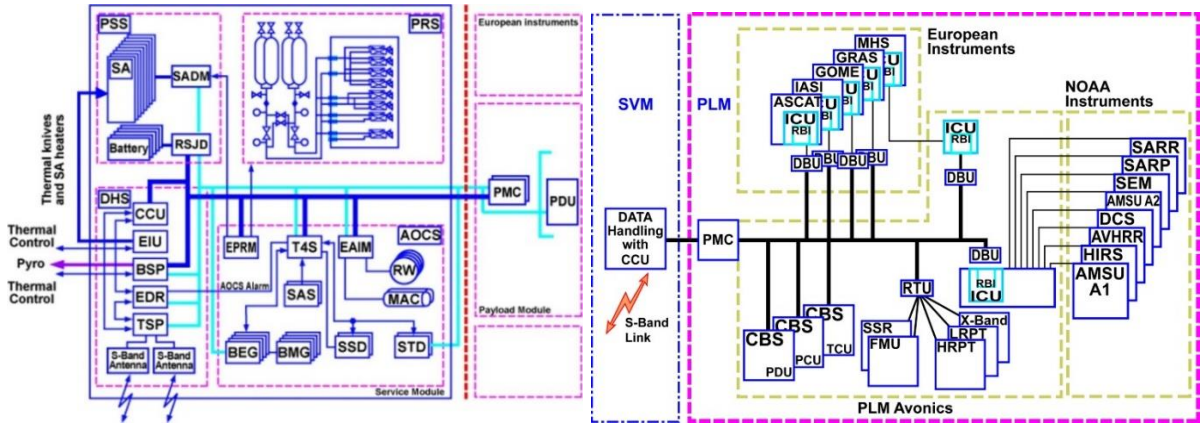

Figure 7.23: MetOp-A decentralised data handling architecture

The **NIU** performs command and control through a **dedicated Instrument Control Unit** (**ICU**) and collects measurement data through a **Digital Signal Processor** (**DSP**). It also compresses the Advanced Very High-Resolution Radiometer (AVHRR) channels. To allow for selective encryption in the **Formatting and Multiplexing Unit** (**FMU**), the NIU provides measurement data to the FMU via four distinct data streams:

- NOAA Interface Unit (NIU)
- Microwave Humidity Sounder (MHS) Protocol conversion Unit (MPU)
- Formatting and Multiplexing Unit (FMU)
- Solid State Recorder (SSR)

The FMU collects measurement data from the various instruments and the NIU and MPU. The interface uses **standard Consultative Committee for Space Data Systems** (**CCSDS**) **formats** and provides switchable encryption functions. The FMU provides at its outputs three different data streams for the various measurement data transmission subsystems and data storage. Global coverage of the measurement data is achieved by **a recording of all measurement data over a complete orbit** from ground station to ground station. A **Solid-State Recorder** (SSR) with a **24 Gbit** storage capacity and a data rate of **70 Mbit/s** is used to do this. **Simultaneous recording and dumping** is supported, such that special measures to avoid data losses during down-link are not required. **At each ground station pass the recorder can be dumped** as far as the actual recording position, i.e., also measurement data acquired during the pass can immediately be downlinked within the same pass. SSR memories are sufficient to provide the necessary internal **redundancies** and to **cover worst case down-link** [7.14].

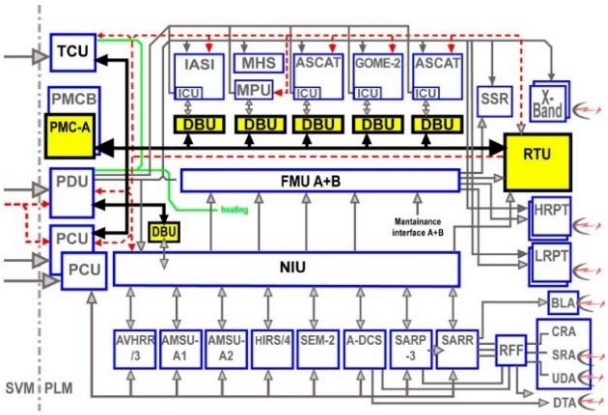

Figure 7.24: Overview of PLM measurement data acquisition, handling, storage and downlink

7.4 Reverse sizing

7.4.1 OBC features as frequency and throughputs by similarity

Components	#	Code (words)	Data (words)	Typical KIPS	Typical frequency	Acquisition frequency	KIPS
ADCS							
RWs	3	1000	300	5	2 Hz	**1 Hz**	**2.5**
Thrusters	16	600	400	1.2	2 Hz	**1 Hz**	**0.6**
Earth sensors	2	1500	800	12	10 Hz	**5 Hz**	**6**
Sun sensors	4	500	100	1	1 Hz	**1 Hz**	**1**
Gyroscopes	4	800	500	9	10 Hz	**5 Hz**	**4.5**
MTs	2	1000	200	1	2 Hz	**1 Hz**	**0.5**
Kinematic integration	1	2000	200	15	10 Hz	**10 Hz**	**15**
Error det.	1	1000	100	12	10 Hz	**10 Hz**	**12**
Attitude det.	1	15000	3500	150	10 Hz	**10 Hz**	**150**
Attitude control	1	24000	4200	60	10 Hz	**10 Hz**	**60**
Complex ephemeris	1	3500	2500	4	0.5 Hz	**0.5 Hz**	**4**
Orbit propagation	1	13000	4000	20	1 Hz	**1 Hz**	**20**
PS							
Tank control valves	12	800	1500	3	0.1 Hz	**0.1 Hz**	**3**
Tank pressure sensors	4	800	1500	3	0.1 Hz	**0.1 Hz**	**3**
EPS							
Power voltage control	1	1200	500	5	1 Hz	**0.1 Hz**	**0.5**
Power current control	1	1200	500	5	1 Hz	**0.1 Hz**	**0.5**
TCS							
Active control (15 heaters)	1	400	750	1.5	0.1 Hz	**0.1 Hz**	**1.5**
TTMTC							
Transponder (uplink)	1	1000	4000	7	10 Hz	**10 Hz**	**7**
Transponder (downlink)	4	1000	2500	3	10 Hz	**10 Hz**	**3**
System (OS)							
I/O device handlers	1	2000	700	50	5 Hz	**1 Hz**	**10**
Test and diagnostic	1	700	400	0.5	0.1 Hz	**0.1 Hz**	**0.5**
Math utilities	1	1200	200	0.5	1 Hz	**1 Hz**	**0.5**
Executive	1	3500	2000	60	10 Hz	**10 Hz**	**60**
Run time kernel	1	8000	4000	60	10 Hz	**10 Hz**	**60**
Complex autonomy	1	15000	10000	20	10 Hz	**10 Hz**	**20**
Fault detection	1	4000	1000	15	5 Hz	**1 Hz**	**3**
Fault correction	1	2000	10000	5	5 Hz	**5 Hz**	**5**

Table 7.15: MetOp-A throughput needed computed by similarity

Considering a preliminary analysis **400% margin** [7.8], we can compute ROM, RAM and throughput MetOp-A OBCs have to provide.

Margined:	ADCS	PS	EPS	TCS	TTMTC	OS	**TOT**
throughput (KIPS)	1565.5	240	5	7.5	95	795	**2708**
code (words)	406500	64000	12000	2000	25000	182000	**691500**
data (words)	131000	120000	5000	3750	70000	141500	**471250**

Table 7.16: total throughput, code and data MetOp-A OBCs have to handle

These results lead to required **ROM = 1383 kb**, **RAM = 2325.5 kb**, **TP = 2.7 MIPS**. These requirements are **split** between **SVM Central Communication Unit** (CCU) and **PLM Payload Module Computer** (PMC). Almost all the data considered in this reverse sizing is handled by the SVM OBCs, that deal with ADCS, PS, EPS, TCS and 2/5 of TTMTC (S-band telemetry downlink and telecommands uplink); PLM OBCs handle the remaining 3/5 of TTMTC (X-band, LRPT and HRPT downlink). But PLM OBCs also deal with the data coming from the scientific instruments, pre-process it and send it continuously to LRPT and HRPT downlink and to the Solid-State Recorder (SSR) storage, and during the communication window with ground station drive it from the SSR to X-band downlink; for this reason, they need extra ROM, RAM and MIPS not calculated in this sizing.

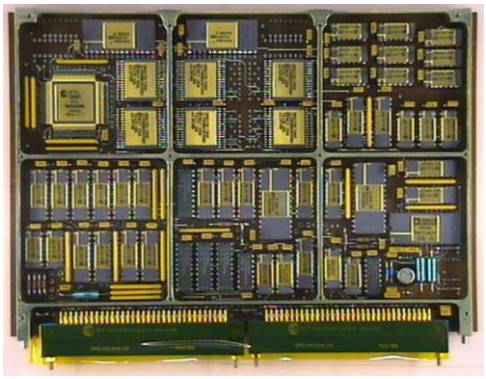

Figure 7.25: MA 31750 based OBC

The SVM CCU mounted on MetOp-A includes a **MA 31750 microprocessor** with two redundant memory modules of **224 Kwords**, that provides **1 MIPS** [16][17]; it is undersized with respect to ROM, RAM and MIPS requirements calculated here. Discrepancy is present because the calculations performed here used **conservative 400% margins**. MetOp-A engineers used less margins due to the similarity of MetOp-A's subsystems components to the flight-proven ones of already existing satellites, and so their actual throughput, data and code requirements were well known.

7.4.2 On board memory size

The **total scientific instruments data rate** is 7.5 kbit/s (ADCS) + 2.1 kbit/s (AMSU-A1/A2) + 60 kbit/s (ASCAT) + 622 kbit/s (AVHRR/3) + 40 kbit/s (GOME-2) + 60 kbit/s (GRAS) + 2.9 kbit/s (HIRS/4) + 1500 kbit/s (IASI) + 3.9 kbit/s (MHS) + 2.4 kbit/s (SARP-3/SARR) + 0.166 kbit/s (SEM-2) = **2301 kbit/s** [15]. Considering an orbital period of 101.4 minutes, the total amount of data collected by MetOp-A scientific instruments in one orbit is **14 Gbit**, that can be stored inside the onboard SSR storage of **24 Gbit** until it's downlinked back to Earth once per orbit.

Bibliography

1. Objectives, Functionalities, Mission Analysis

[1.1] eoPortal, MetOp (Meteorological Operational Satellite Program of Europe)

[1.2] ESA, MetOp

[1.3] K. Merz, M. A. Martín Serrano, D. Kuijper, M.A. García Matatoros: "The MetOp-A orbit acquisition strategy and its leop operational experience", ESA/ESOC, 2007

[1.4] François Spoto, Yves Bordes, Simon Chalkley, Luis Huertas, Omar Sy, Yves Buhler, Jean-Michel Caujolle: "Preparing MetOp for Work, Launch, Early Operations and Commissioning", ESA/ESTEC, EUMETSAT, ESA bulletin 127, August 2006

[1.5] P.G Edwards, D. Pawlak: "Metop: The Space Segment for Eumetsat's Polar System", ESA/ESTAC, Matra Marconi Space, ESA bulletin 102, May 2000

[1.6] Pierluigi Righetti, Jose Maria de Juana Gamo, Richard Dyer: "Mission analysis of MetOp-A end-of-life operations", EUMETSAT, 2012

[1.7] European Cooperation for Space Standardization (ECSS), Standards

2. Propulsion Subsystem

[2.1] eoPortal, MetOp (Meteorological Operational Satellite Program of Europe)

[2.2] ESA, MetOp

[2.3] K. Merz, M. A. Martín Serrano, D. Kuijper, M.A. García Matatoros: "The MetOp-A orbit acquisition strategy and its leop operational experience", ESA/ESOC, 2007

[2.4] European Cooperation for Space Standardization (ECSS), Standards

[2.5] Trading Economics, Commodities - live quote price trading data

[2.6] SatCatalog: Moog MONARC-22-6

3. Tracking, Telemetry and Telecommand Subsystem

[3.1] eoPortal, MetOp (Meteorological Operational Satellite Program of Europe)

[3.2] ESA, MetOp

[3.3] European Cooperation for Space Standardization (ECSS), Standards

[3.4] ESA, Managing signals at the top of the world

[3.5] Observing Systems Capability Analysis and Review Tool OSCAR, Satellite: Metop-A

[3.6] EUMETSAT, EPS-SG (Metop-SG) Direct Data Broadcast (DDB) Radio Frequency (RF) Space to Ground Interface Control Document (ICD)

[3.7] Space System Engineering and Operations, Tracking Telemetry & Telecommand s\s, Prof. Michèle Lavagna, A.A.2022/23 lecture notes

[3.8] Space System Engineering and Operations, Exercise Session: Telecommunication System (TMTC), Andrea Brandonisio, Prof. Michèle Lavagna, A.A.2022/23

[3.9] ESA, MetOp technical summary

[3.10] P.G Edwards, D. Pawlak: "Metop: The Space Segment for Eumetsat's Polar System", ESA/ESTAC, Matra Marconi Space, ESA bulletin 102, May 2000

[3.11] Christelle Crozat, Pier-Luigi Righetti, Lionel de la Taille, Frank Perlik and Peter Collins, MetOp-A Attitude and Orbit Control Operations, "MetOp-A Attitude and Orbit Control Operations", SpaceOps 2008 Conference (Hosted and organized by ESA and EUMETSAT in association with AIAA)

4. Attitude and Orbit Control Subsystem

[4.1] eoPortal, MetOp (Meteorological Operational Satellite Program of Europe)

[4.2] ESA, MetOp

[4.3] European Cooperation for Space Standardization (ECSS), Standards

[4.4] Space System Engineering and Operations, Attitude\orbit determination & Control, Prof. Michèle Lavagna, A.A.2022/23 lecture notes

[4.5] Space System Engineering and Operations, Exercise Session: Attitude Determination and Control System (ADCS), Andrea Brandonisio, Prof. Michèle Lavagna, A.A.2022/23

[4.6] Christelle Crozat, Pier-Luigi Righetti, Lionel de la Taille, Frank Perlik and Peter Collins, MetOp-A Attitude and Orbit Control Operations, "MetOp-A Attitude and Orbit Control Operations", SpaceOps 2008 Conference (Hosted and organized by ESA and EUMETSAT in association with AIAA)

[4.7] Francisco SANCHO, Jörg FISCHER and Stefania TARQUINI, "Non-nominal Attitude Manoeuvres during Metop-A extended Lifetime"

[4.8] P.G Edwards, D. Pawlak: "Metop: The Space Segment for Eumetsat's Polar System", ESA/ESTAC, Matra Marconi Space, ESA bulletin 102, May 2000

[4.9] SatCatalog: Sodern STD 16

[4.10] SatCatalog: Adcole Maryland Aerospace Digital Sun Sensor

[4.11] ESA: TNO Coarse Sun Sensor using European cells

[4.12] SatCatalog: LH3Harris technologies CIRUS

[4.13] SatCatalog: Bradford Space W18

[4.14] SatCatalog: ZARM Technik AG MT400-2

[4.15] SatCatalog: Moog MONARC-22-6

[4.16] ESA pointing error engineering handbook, 2011

5. Thermal Control Subsystem

[5.1] eoPortal, MetOp (Meteorological Operational Satellite Program of Europe)

[5.2] ESA, MetOp

[5.3] European Cooperation for Space Standardization (ECSS), Standards

[5.4] Space System Engineering and Operations, Thermal Control subsystem, Prof. Michèle Lavagna, A.A.2022/23 lecture notes

[5.5] Space System Engineering and Operations, Exercise Session: Thermal Control System (TCS), Andrea Brandonisio, Prof. Michèle Lavagna, A.A.2022/23

[5.6] ESA, MetOp, Service Module thermal control

[5.7] ESA, MetOp, Payload Module thermal control

[5.8] MT Aerospace, Spacecraft propellant tanks

[5.9] SatCatalog: Sodern STD 16

[5.10] SatCatalog: Adcole Maryland Aerospace Digital Sun Sensor

[5.11] ESA: TNO Coarse Sun Sensor using European cells

[5.12] SatCatalog: LH3Harris technologies CIRUS

[5.13] SatCatalog: Bradford Space W18

[5.14] SatCatalog: ZARM Technik AG MT400-2

[5.15] SatSearch: LP 33450 43Ah Space Cell

[5.16] Douglas Felipe da Silva, Ezio Castejon Garcia: "Experimental determination of the effective thermal properties of a multi-layer insulation blanket", 22nd International Congress of Mechanical Engineering (COBEM 2013)

[5.17] Thermal Engineer, Multi-Layer Insulation (MLI)

[5.18] Sapienza Università di Roma, Consiglio d'Area di Ingegneria Aerospaziale: "Steady state heat transmission in a multi-layer insulation (MLI)"

[5.19] Heavens Above, MetOp-A - orbit

[5.20] Romain Peyrou-Lauga, "Using real Earth Albedo and Earth IR Flux for Spacecraft Thermal Analysis", ESA, ESTEC, 47th International Conference on Environmental Systems ICES-2017-142, 16-20 July 2017

[5.21] NASA, Jet Propulsion Laboratory, California Institute of Technology, "NASA Spacecraft Maps Earth's Global Emissivity"

[5.22] National Oceanic and Atmospheric Administration NOAA, "Climate Change: Global Temperature"

[5.23] R. J. Turner, E. A. Taylor, J. A. M. McDonnell, H. Stokes, P. Marriott, J. Wilkinson, D. J. Catling, R. Vignjevic, L. Berthoud, M. Lambert, "Cost effective honeycomb and multi-layer insulation debris shields for unmanned spacecraft", International Journal of Impact Engineering, Volume 26, Issues 1–10, December 2001, Pages 785-796

[5.24] NASA Johnson Space Center, "Silver-Teflon coating improvement"

[5.25] Demezzi, Kapton 200 HN

[5.26] Sheldahl, ITO Coated Silver FEP

[5.27] Minco Thermal Solutions Design Guide

[5.28] Space System Engineering and Operations, Exercise Session: On-Board Data Handling System (OBDH), Andrea Brandonisio, Prof. Michèle Lavagna, A.A.2022/23

6. Electric Power Subsystem

[6.1] eoPortal, MetOp (Meteorological Operational Satellite Program of Europe)

[6.2] ESA, MetOp

[6.3] European Cooperation for Space Standardization (ECSS), Standards

[6.4] Space System Engineering and Operations, Electric power generation & Storage subsystem, Prof. Michèle Lavagna, A.A.2022/23 lecture notes

[6.5] Space System Engineering and Operations, Exercise Session: Electrical Power System (EPS), Andrea Brandonisio, Prof. Michèle Lavagna, A.A.2022/23

[6.6] ESA, MetOp, Service Module electrical power

[6.7] ESA, MetOp, Service Module power buses

[6.8] ESA, MetOp, Payload Module electrical power, distribution, control and harness

[6.9] Lisa M. Hague, Kenneth J. Metcalf, George M. Shannon, Robert C. Hill, and Cheng-Yi Lu: "Performance of international space station electric power system during station assembly", IECEC 96. Proceedings of the 31st Intersociety Energy Conversion Engineering Conference, 11-16 Aug. 1996

[6.10] AZUR SPACE: Silicon Solar Space Cell S 32

[6.11] CESI: Triple-Junction Solar Cell for Space Applications (CTJ30)

[6.12] Nikola Papež, Rashid Dallaev, Ştefan Ţălu, and Jaroslav Kaštyl: "Overview of the Current State of Gallium Arsenide-Based Solar Cells", Materials (Basel), 2021

[6.13] University WAFER: Pros and Cons of Gallium Arsenide Solar Cells

[6.14] Space System Engineering and Operations, Exercise Session: On-Board Data Handling System (OBDH), Andrea Brandonisio, Prof. Michèle Lavagna, A.A.2022/23

7. Configuration and On-Board Data Handling Subsystem

[7.1] eoPortal, MetOp (Meteorological Operational Satellite Program of Europe)

[7.2] ESA, MetOp, Satellite Overall Configuration

[7.3] ESA, MetOp, Payload Module

[7.4] ESA, MetOp, Service Module structure

[7.5] ESA, MetOp, Service Module configuration

[7.6] ESA, MetOp, Service Module structural support

[7.7] Arianespace: "Soyuz at the Guiana Space Centre", User's Manual, Issue 2 – Revision 0, March 2012

[7.8] European Cooperation for Space Standardization (ECSS), Standards

[7.9] Space System Engineering and Operations, Exercise Session: Configuration System (CONF), Andrea Brandonisio, Prof. Michèle Lavagna, A.A.2022/23

[7.10] Space System Engineering and Operations, On Board Data Handling subsystem, Prof. Michèle Lavagna, A.A.2022/23 lecture notes

[7.11] Space System Engineering and Operations, Exercise Session: On-Board Data Handling System (OBDH), Andrea Brandonisio, Prof. Michèle Lavagna, A.A.2022/23

[7.12] ESA, MetOp, Service Module data handling

[7.13] ESA, MetOp, Payload Module command, control and communication

[7.14] ESA, MetOp, Payload Module measurement data acquisition, handling, storage

[7.15] ESA, MetOp technical summary

[7.16] Datasheet catalogue, Dynex Semiconductor: MA31750 - High Performance MIL-STD-1750 Microprocessor

[7.17] ESA microelectronics, SYDERAL SA: "Past, present and future microprocessor needs at SYDERAL"

Appendix A: MATLAB code

Propulsion Subsystem

```
%% Propulsion system sizing
clc; close all; clearvars;

flag_pres_gas = 0; % 0 for using He; 1 for N2
flag_material = 1; % 0 for Ti; 1 for Al
flag_shape = 1; % 0 for spherical; 1 for cylindrical

m_dry = 3769; % [Kg]
m_fin = 1.2 * m_dry;

Dv = 166 + 0.2 * 166; % Dv + 20% of margin [m/s]

% Specific impulse
I = 230; % [s]

% Density of Hydrazine
rho = 1.01 * 1e3; % [kg/m^3]
g = 9.81; % [m/s^2]
MR = exp(Dv/(I * g)); % Mass ratio [-]

m_in = MR * m_fin;
m_prop = m_in - m_fin;
m_prop = m_prop + 0.055 * m_prop; % 5.5% of margin

% Compute the volume of Hydrazine
V_prop = m_prop/rho; % [kg]
V_prop = V_prop + 0.1 * V_prop; % Adding 10%

if flag_pres_gas == 0
    R = 2077.3; % [J/kg K]
    gamma = 1.67;
end
if flag_pres_gas == 1
    R = 296.8;
    gamma = 1.40;
end

% Blow Down system (B = 4-6)

B = 5; % B = P_gas_in/ P_gas_fin
Dp_feed = 0.05; % MPa
P_chamb = 1; % MPa
DP_inj = 0.3 * P_chamb;
P_tank_f = P_chamb + DP_inj + Dp_feed;
P_gas_f = P_tank_f;

V_gas_in = V_prop/(B-1); % Isothermal transformation
V_gas_fin = B * V_gas_in;
```

```
P_gas_in = B * P_gas_f;
T_tank = 293; % [K]

P_tank_in = B * P_tank_f;
V_tank = V_gas_in + V_prop;
V_tank = V_tank / 4; % Number of tanks
V_tank = V_tank + 0.01 * V_tank; % 1% of margin for bladder

m_press = (P_tank_in * 1e6 * V_gas_in)/(R * T_tank);
m_press = m_press + 0.2 * m_press; % 20% of margin

switch flag_material
    case 0
    rho_tank = 2780; % [kg/m^3]
    sigma_tank = 950; % [MPa]

    case 1
    rho_tank = 2810; % [kg/m^3]
    sigma_tank = 503; % [MPa]
end

switch flag_shape
    case 0
    r_tank = (3 * V_tank/(4 * pi))^(1/3);
    t_tank = (P_tank_in * r_tank)/(2 * sigma_tank);
    m_tank = rho_tank * (4/3) * pi * ((r_tank + t_tank)^3 - r_tank^3);

    case 1
    h = linspace(0.1,2,100); % length of cylindrical tank from 10 cm to 2 m
    r_tank = sqrt(V_tank./(pi .* h));
    t_tank = (P_tank_in .* r_tank)/( sigma_tank);
    m_tank = rho_tank .* pi .* h .* ((r_tank + t_tank).^2 - r_tank .^2);
end

   % Thrusters MONARC 22-6
   m_thr = 0.72 * 16;

   m_PS = m_tank * 4 + m_press + m_thr;
   m_PS = m_PS + 0.1 * m_PS;
```

Tracking, Telemetry and Telecommand Subsystem

X band

```
clc; close all; clearvars;

R = 70000000; % 70 Mbps, bps
Xdl = 7.8; % downlink, GHz
XP = 90; % power, W
Xd = 0.1; % diameter, m
```

```
% transmitted power
mu_amp = 0.56; % efficiency of the amplifier (TWTA at 90 W)
Ptx = mu_amp * XP;
Ptx_dbW = 10*log10(Ptx); % power in dbW

% modulation
a_QPSK = 2;
% encoding (Reed-Solomon)
Eb_N0_min = 5.5; % minimum Eb/N0 for R-S with BER=10^-5, dB
a_RS = 1.14;
R = R*a_RS/a_QPSK;

% satellite antenna
mu_par = 0.55; % efficiency of parabolic antenna
c = 300000000; % speed of light, m/s
lambda = c/(Xdl*1e9); % wavelength, m
G_ant = 10*log10(pi*Xd^2*mu_par/lambda^2); % antenna gain

% ground station
D_ant = 11; % Svalbard ground station X-band antenna diameter, m
G_rx = 10*log10(pi*D_ant^2*mu_par/lambda^2); % ground antenna gain, dB
th_rx = 65.3*lambda/D_ant; % beamwidth, deg

% losses
l_cable = -1; % cable losses, between -1 and -3 dB
r = 2890000; % Slant range, m
l_space = 20*log10(lambda/(4*pi*r)); % free space losses, dB
l_point = -1; % pointing losses, dB
l_atm = -3.85; % atmospheric losses from charts, dB

% Effective Isotropic Radiated Power
EIRP = Ptx_dbW+G_ant+l_cable; % dB

% received power
P_rx = EIRP+G_rx+l_space+l_atm+l_point; % dB

% System Noise Density
k = 1.38e-23; % Boltzmann constant, Ws/K
Ts = 250; % sensor temperature, K
N0 = 10*log10(k*Ts); % dB

% error per bit to noise density ratio
Eb_N0 = P_rx-N0-10*log10(R)
Eb_N0_min = Eb_N0_min + 3 % Eb/N0 min + 3 dB margin

disp('Eb_N0 must be higher than Eb_N0_min')

%% carrier modulation index reduction
B_mod = 60*pi/180; % Modulation index, 60 deg for normal-mode downlink bit rates
P_mod_loss = 20*log10(cos(B_mod)); % dB
P_carrier = P_rx+P_mod_loss; % carrier power, dB
```

```
% signal to noise ratio SNR
B = 63000000; % bandwidth, Hz
SNR_carrier = P_carrier - N0 - 10*log10(B); % dB
SNR_min = 10; % minimum SNR depending on the ground station constraints
SNR_margin = SNR_carrier-SNR_min % dB

disp('SNR_margin must be higher than 3 dB')
```

S band

```
clc; close all; clearvars;

Sul = 2053.4583; % uplink, MHz
Sdl = 2230; % downlink, MHz
R_ul = 2000; % data rate uplink, bit/s
R_dl = 4096; % data rate downlink, bit/s
SP = 30; % input power, W
Sd = 0.115; % correspondent parabolic antenna diameter, m

% Transmitted power
mu_amp = 0.15; % efficiency of the amplifier (SSA at 30 W)
Ptx = mu_amp*SP; % W
Ptx_dbW = 10*log10(Ptx); % dbW
Ptx_ul = 20000; % ground station transmitted power, W
Ptx_ul_dbW = 10*log10(Ptx_ul); % dbW

% bit error rate
BER_ul = 1e-7; % uplink
BER_dl = 1e-5; % downlink

% modulation
a_QPSK = 2;
% encoding (Reed-Solomon)
Eb_N0_min = 5.5; % minimum Eb/N0 for R-S with BER=10^-5, dB
a_RS = 1.14;

% Real data rates
R_ul = R_ul*a_RS/a_QPSK; % kbit/s
R_dl = R_dl*a_RS/a_QPSK; % kbit/s

% satellite antenna
mu_par = 0.55; % efficiency of parabolic antenna
c = 300000000; % speed of light, m/s
lambda_ul = c/(Sul*1e6); % uplink wavelength, m
lambda_dl = c/(Sdl*1e6); % downlink wavelength, m
G_ant_ul = 10*log10(pi*Sd^2*mu_par/lambda_ul^2); % uplink antenna gain, dB
G_ant_dl = 10*log10(pi*Sd^2*mu_par/lambda_dl^2); % downlink antenna gain, dB

% ground station
D_ant = 11; % Svalbard ground station S-band antenna diameter, m
G_rx_ul = 10*log10(pi*D_ant^2*mu_par/lambda_ul^2); % ground antenna gain (uplink), dB
G_rx_dl = 10*log10(pi*D_ant^2*mu_par/lambda_dl^2); % ground antenna gain (downlink),dB
```

```
th_rx_ul = 65.3*lambda_ul/D_ant; % beamwidth (uplink), deg
th_rx_dl = 65.3*lambda_dl/D_ant; % beamwidth (downlink), deg

% Losses
l_cable = -1; % cable losses, between -1 and -3 dB
r = 2890000; % Slant range, m
l_space_ul = 20*log10(lambda_ul/(4*pi*r)); % free space losses (uplink), dB
l_space_dl = 20*log10(lambda_dl/(4*pi*r)); % free space losses (downlink), dB
eta = 0.01; % pointing accuracy, dB
l_point_ul = -12*(eta/th_rx_ul)^2; %pointing losses (uplink), dB
l_point_dl = -12*(eta/th_rx_dl)^2; %pointing losses (uplink), dB
l_atm_ul = -0.4; % atmospheric losses (uplink), dB
l_atm_dl = -0.4; % atmospheric losses (downlink), dB

% Effective Isotropic Radiated Power
EIRP_ul = Ptx_ul_dbW+G_rx_ul+l_cable; % uplink, dB
EIRP_dl = Ptx_dbW+G_ant_dl+l_cable; % uplink, dB

% Received power
P_rx_ul = EIRP_ul+G_ant_ul+l_space_ul+l_atm_ul+l_point_ul; % uplink, dB
P_rx_dl = EIRP_dl+G_rx_dl+l_space_dl+l_atm_dl+l_point_dl; % uplink, dB

% System Noise Density
k = 1.38e-23; % Boltzmann constant, Ws/K
Ts = 250; % sensor temperature, K
N0 = 10*log10(k*Ts); % dB

% Error per bit to noise density ratio
Eb_N0_ul = P_rx_ul-N0-10*log10(R_ul) %uplink
Eb_N0_dl = P_rx_dl-N0-10*log10(R_dl) %downlink
Eb_N0_min = Eb_N0_min + 3 % Eb/N0 min + 3 dB margin
disp('Eb_N0 must be higher than Eb_N0_min')

% carrier modulation index reduction
B_mod_ul = 78*pi/180; % Modulation index (uplink), rad
B_mod_dl = 60*pi/180; % Modulation index (downlink), rad
P_mod_loss_ul = 20*log10(cos(B_mod_ul)); % uplink, dB
P_mod_loss_dl = 20*log10(cos(B_mod_dl)); % uplink, dB
P_carrier_ul = P_rx_ul+P_mod_loss_ul; % carrier power (uplink), dB
P_carrier_dl = P_rx_dl+P_mod_loss_dl; % carrier power (downlink), dB

% signal to noise ratio SNR
B_ul = 1500000; % uplink bandwidth (TC&ranging), Hz
B_dl = 2000000; % downlink bandwidth (TM), Hz
SNR_carrier_ul = P_carrier_ul - N0 - 10*log10(B_ul); % uplink, dB
SNR_carrier_dl = P_carrier_dl - N0 - 10*log10(B_dl); % uplink, dB
SNR_min = 10; % minimum SNR depending on the ground station constraints
SNR_margin_ul = SNR_carrier_ul-SNR_min % dB
SNR_margin_dl = SNR_carrier_dl-SNR_min % dB

disp('SNR_margin must be higher than 3 dB')
```

Attitude and Orbit Control Subsystem

```
%% AOCS system sizing
clc; close all; clear;

% Reaction wheels
h = 40; % Nms
Trw = 0.248; % Nm

% Thrusters
Isp = 230; % s
L = 1.25; % force arm, m
F = 22.7; % N

% Gravity Gradient data
% launch shape: 6.2 m * 2.5 m * 2.5 m
m = 4085; % mass, kg
Ix = (1/12) * m * (2.5^2 + 2.5^2); % kg*m^2
Iy = (1/12) * m * (6.2^2 + 2.5^2); % kg*m^2
Iz = (1/12) * m * (6.2^2 + 2.5^2); % kg*m^2
Imax = Iz; % kg*m^2
Imin = Ix; % kg*m^2
th_max = 0.17*pi/180; % max deviation of z axis from radial direction to the planet,
rad
mu_earth = 3.986e5; % km^3/s^2

% Orbit
a = 7188; % km
e = 0.0195159;
b = a * sqrt(1 - e^2); % mean radius, km
R = sqrt(a * b); % A_ellipse = A_circle -> equivalent circle radius, km

% Solar Radiation Pressure data
cp_cg = 0.3; % distance between satellite center of solar pressure and of gravity, m
Fs = 1373; % Sun heat flux at Earth, W/m^2
Asp = 6.2 * 2.5; % m^2
q = 0.5; % body reflectivity coefficient (0<q<1, typically 0.5-0.6)

%% Disturbance torques

% GG
T_GG = (3 * mu_earth / (2 * R^3)) * (Imax - Imin) * sin (2 * th_max); % Nm

% SRP
I = 0; % worst case scenario incidence angle
c = 300000000; % speed of light, m/s
T_SRP = (Fs / c) * Asp * (1 + q) * cos(I) * (cp_cg); % Nm

% Magnetic
M = 7.96*1e15;              % Tm^3, half of earth magnetic moment on the equator
B = 2*M/((R*1000)^3);       % earth magnetic field
D = 5;                      % Am^2, residual dipole on s/c, range[1-20]
```

```
T_magn = D*B;              % Nm

% Drag
rho = 1.13*1e-14;  % kg/m^3, from 09_attitudeslides_chart
cd = 2.2;
mu = 398600*1e9;   % m^3/s^2
A_drag = 6.3*2.5;  % assuming dimensions of launch config
v = sqrt(mu/R);    % approx circular
cpa_cg = 2.5/2;
T_drag = 1/2*rho*cd*A_drag*(v^2)*cpa_cg; % Nm

% margin for preliminary estimation / statistical = 100%
T_dist = 2 * (T_GG + T_SRP + T_drag + T_magn); % Nm

%% Actuators: reaction wheels

% Disturbances rejection
T_op = 2 * pi * sqrt(a^3 / mu_earth); % orbital period, s
h_dist_period = T_dist * T_op; % Nms
desat = h / h_dist_period; % number of orbit after which desaturation is needed

% Slew maneuver of th_m = 180° around max axis of inertia, worst case
th_m = 180;
th_dot_max = 0.5; % max slew rate
t = th_m / th_dot_max;
T_slew = 4 * (th_m*pi/180) * Imax / t^2; % > Trw -> can't slew with this rate

% max affordable slew rate
t_min = sqrt(4 * (th_m*pi/180) * Imax / Trw);
th_dot_max_ach = th_m / t_min; % deg/s

%% Thrusters

% Reaction Wheels desaturation
n = 2; % number of thrusters
t_burn = h / (n * L * F); % s
t_desat = t_burn; % s
% We prefer higher desaturation time
t_desat_imposed = 5; % s
F_des = h / (n * L * t_desat_imposed); % thrust to desaturate in 5 seconds, N

% Propellant mass
g0 = 9.81;
m_prop_1rw = t_desat_imposed * F_des / (Isp * g0); % to desaturate 1 RW, kg
deltat_des = T_op * desat; % desaturate each desat orbits, s
lifetime = 5 * 365 * 24 * 60 * 60; % s
N_RW = 3;
m_prop_des = N_RW * m_prop_1rw * lifetime / deltat_des; % total propellant mass to
desaturate, kg

% Magnetotorquers
D_nec = T_dist/B; % dipole necessary to counteract disturbances
```

Thermal Control Subsystem

```
clear all; close all; clc

%% Variables
SC_mat = 0; % 0 = MLI, 1 = aluminized Kapton, 2 = polished metal, 3 = Al/FEP, 4 = beta
cloth
rad_mat = 0; % 0 = silver teflon

%% MetOp-A
e = 0.0194701; % orbit eccentricity [5.19]
l1 = 6.3; % m
l2 = 2.5; % m
l3 = 2.5; % m, launch configuration not to consider solar array (own TCS),
            % instruments (own TCS), antennas (wide T range)
R_pl = 6371; % km
R_med = R_pl + 824; % km
p = R_med*(1+e*cos(45*pi/180)); % km
Rp = p/(1+e); % pericentre, km
Ra = p/(1-e); % apocentre, km

T_min = 273+15; % min s/c temperature, 15 degrees margin, K
Q_int_min = 1500; % internal power generated, cold case, W
T_max = 314-15; % max s/c temperature, 15 degrees margin, K
Q_int_max = 2000; % internal power generated, hot case, W
K_E = 1; % Diffusion factor [5.20]

% equivalent sphere
A_tot = 2*(l1*l2 + l1*l3 + l2*l3);
r_sphere = sqrt(A_tot/(4*pi));

% Solar flux
q0 = 1367.5; % W/m^2, solar flux at 1 AU (Earth)
q_sun = q0; % distance sc-sun = distance earth-sun

% Albedo
alb = 0.35; % Earth albedo [5.20]
theta = 0; % irradiance angle between s/c and planet
q_alb_max = q_sun*alb*cos(theta)*(R_pl/Rp)^2; % W/m^2
q_alb_min = q_sun*alb*cos(theta)*(R_pl/Ra)^2; % W/m^2

% Infrared
sigma = 5.67e-8; % W/m^2 K^4
eps_E = 0.95; % Earth emissivity [5.20][5.21]
T_pl = 13.9 + 0.86 + 273.15; % K [5.22]
q_IR_max = sigma*eps_E*T_pl^4*(R_pl/Rp)^2;
q_IR_min = sigma*eps_E*T_pl^4*(R_pl/Ra)^2;

%% HOT CASE
switch SC_mat
    case 0
        eps = 0.02; % MLI effective emissivity [5.16]
```

```
        alpha = 0.004; % MLI effective absorptivity [5.16]
    case 1
        eps = 0.6; % Al kapton emissivity [5.4][5.5]
        alpha = 0.4; % Al kapton absorptivity [5.4][5.5]
    case 2
        eps = 0.1; % polished metal (Al alloy) emissivity [5.4][5.5]
        alpha = 0.2; % polished metal (Al alloy) absorptivity [5.4][5.5]
    case 3
        eps = 0.78; % Al/FEP emissivity [5.4][5.5]
        alpha = 0.13; % Al/FEP absorptivity [5.4][5.5]
    case 4
        eps = 0.8; % beta cloth emissivity [5.4][5.5]
        alpha = 0.4; % beta cloth absorptivity [5.4][5.5]
end

h_min = Rp-R_pl; % Min altitude, km
F_max = 0.5*(1-sqrt((h_min/R_pl)^2+2*h_min/R_pl)/(1+h_min/R_pl)); % view factor

% Q sun
A_cross = pi*r_sphere^2;
Q_sun = A_cross*alpha*q_sun; % W

% Q albedo
Q_alb_max = A_tot*F_max*alpha*K_E*q_alb_max;

% Q infrared
Q_IR_max = A_tot*F_max*q_IR_max;

% Tsc from heat balance Qemitted=Qint+Qsun+Qalb+Qirr
T_sc_hot = ((Q_int_max+Q_sun+Q_alb_max+Q_IR_max)/(sigma*eps*A_tot))^(1/4) % s/c
temperature, K

if T_sc_hot > T_max
    disp('T_sc_hot > T_max, temperature outside the range, a cooler must be
             introduced')
    % Radiators sizing
    switch rad_mat
        case 0
            eps_rad = 0.8; % silver teflon rediators emissivity [5.4][5.5]
            alpha_rad = 0.09; % silver teflon rediators absorptivity [5.4][5.5]
    end

    Q_tot_max = Q_int_max+Q_sun+Q_alb_max+Q_IR_max;
    A_rad_min = (Q_tot_max-sigma*eps*A_tot*T_max^4)/(sigma*(eps_rad-eps)*T_max^4) %
       radiators surface, m^2
    A_e = A_tot-A_rad_min; % area not covered by radiators
end

%% COLD CASE
h_max = Ra-R_pl; % Max altitude, km
F_min = 0.5*(1-sqrt((h_max/R_pl)^2+2*h_max/R_pl)/(1+h_max/R_pl)); % Min view factor
Q_IR_min = A_tot*F_min*q_IR_min;
```

```
T_sc_cold = ((Q_int_min+Q_IR_min)/(sigma*(eps*A_e+eps_rad*A_rad_min)))^(1/4) % s/c
temperature, K

if T_sc_cold < T_min
    disp('T_sc < T_min, a heater must be introduced')
    % heaters sizing
    Q_heaters = sigma*(eps*A_e+eps_rad*A_rad_min)*T_min^4 - Q_IR_min - Q_int_min
end
```

Electric Power Subsystem

```
%% MetOp-A EPS system sizing

clc; close all; clearvars;

%% Variables
SC_mat = 0; % 0 = Si, 1 = Triple Junction Solar Cells InGaP/GaAs/Ge
BAT_mat = 0; % 0 = Li-ion, 1 = Ni-Cd

%% Variable Initialization
% max power requirements of system
P_day = 1810; % W
P_eclipse = 1810; % W

% voltage
V_sys = 28; % V

% time info
T_day = 67*60; % s
T_eclipse = 34*60; % s
T_life = 5; % years

% line efficiencies
x_d = 0.8; % in daylight
x_e = 0.6; % in eclipse

% irradiance
I0 = 1361; % irradiance of Earth, W/m^2
theta = 30; % inclination angle, worst case 30 deg

switch SC_mat
    case 0
        % performance of ISS silicon solar cells
        E_bol = 0.145; % beginning of life efficiency
        dpy = 0.028; % degradation/year
        I_d = 0.7; % inherent degredation
        % t = 0.05; % thickness, cm
        % rho = 75; % density, kg/m^3
        avw = 320; % average weight, g/m^2
        A_cell = 0.0064; % cell area, m^2
```

```
        V_sa_cell = 0.628; % cell voltage, V
    case 1
        % performance of CESI CTJ30 Triple Junction Solar Cells InGaP/GaAs/Ge
        E_bol = 0.295; % beginning of life efficiency
        dpy = 0.0375; % degradation/year
        I_d = 0.7; % inherent degredation
        avw = 890; % average weight, g/m^2
        A_cell = 0.003015; % cell area, m^2
        V_sa_cell = 2.61; % cell voltage, V
end

% battery sizing info (source: slides tables)
N_bat = 5; % number of batteries
C_bat = 40; % battery capacity, Ah

switch BAT_mat
    case 0
        % Li-ion
        DOD = 0.25; % depth of discharge (5 years in LEO)
        eta_bat = 0.4; % transmission efficiency between batteries and load
        E_m = 140; % Wh/kg specific energy
        E_v = 250; % Wh/dm^3 energy density
        V_bat_cell = 3.6; % cell voltage, V
        mu = 0.8; % package efficiency
    case 1
        % Ni-Cd
        DOD = 0.2; % depth of discharge (5 years in LEO)
        eta_bat = 0.4; % transmission efficiency between batteries and load
        E_m = 40; % Wh/kg specific energy
        E_v = 90; % Wh/dm^3 energy density
        V_bat_cell = 1.35; % cell voltage, V
        mu = 0.8; % package efficiency
end

%% Power request to solar array
% in max power demand condition
P_sa = ((P_eclipse * T_eclipse) / (x_e * T_day)) + (P_day / x_d)

%% Specific Power
P0 = E_bol * I0; % specific power output
P_bol = P0 * I_d * cosd(theta); % SA specific power

L_life = (1 - dpy)^T_life;
P_eol = L_life * P_bol;

%% Physical Measurements of SA
A_sa = P_sa / P_eol;
% m_sa = A_sa * rho_si * t

N_cells = ceil(A_sa / A_cell);
N_sa_series = ceil(V_sys / V_sa_cell);
N_real = ceil(N_cells / N_sa_series) * N_sa_series;
```

```
A_sa_real = N_real * A_cell
m_cells = A_sa_real * avw / 1000

%% Battery sizing
% T_r and P_r taken for eclipse
P_r = P_eclipse; % W
T_r = T_eclipse / 3600; % h
C = (T_r * P_r) / (DOD * N_bat * eta_bat);

m_bat = C / E_m
V_bat = C / E_v

N_bat_series = ceil(V_sys / V_bat_cell);
V_real = N_bat_series * V_bat_cell;
C_string = mu * C_bat * V_real;

N_parallel = ceil(C/C_string);
C_real = N_parallel * C_string;
```